



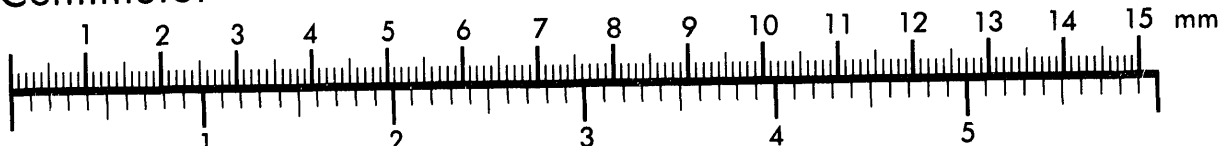
**AIIM**

**Association for Information and Image Management**

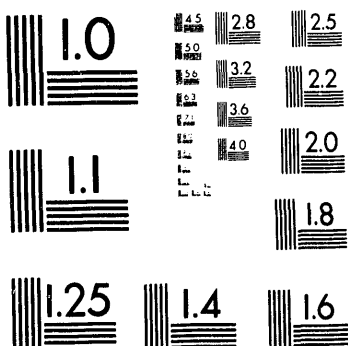
1100 Wayne Avenue, Suite 1100  
Silver Spring, Maryland 20910

301/587-8202

**Centimeter**



**Inches**



MANUFACTURED TO AIIM STANDARDS  
BY APPLIED IMAGE, INC.

1 of 1

Metals and Ceramics Division

**ALLOY DEVELOPMENT OF FeAl ALUMINIDE ALLOYS  
FOR STRUCTURAL USE IN CORROSIVE ENVIRONMENTS**

C. T. Liu  
V. K. Sikka  
C. G. McKamey

Manuscript Prepared-September 1990  
Date Published-February 1993

NOTICE: This document contains information of a preliminary nature. It is subject to revision or correction and therefore does not represent a final report.

Prepared for the  
U.S. Department of Energy  
Assistant Secretary for Conservation and Renewable Energy  
Office of Industrial Technologies  
Advanced Industrial Concepts Materials Program  
ED 38 02 00 0

Prepared by the  
OAK RIDGE NATIONAL LABORATORY  
Oak Ridge, Tennessee 37831-6285  
managed by  
MARTIN MARIETTA ENERGY SYSTEMS, INC.  
for the  
U.S. DEPARTMENT OF ENERGY  
under contract DE-AC05-84OR21400

MASTER

## TABLE OF CONTENTS

	<u>Page</u>
LIST OF FIGURES .....	v
LIST OF TABLES .....	ix
ABSTRACT .....	1
1. INTRODUCTION .....	2
2. STUDY OF BINARY FeAl ALLOYS .....	3
3. EFFECT OF ALLOY ADDITIONS ON STRUCTURE AND PROPERTIES OF Fe-35.8% Al .....	8
3.1 Cr EFFECT .....	9
3.2 B AND Zr EFFECTS .....	9
3.3 Cr EFFECTS IN FA-342 (Fe-35.8Al-0.1Zr-0.24B, at. %) TYPE ALLOYS .....	17
3.4 EFFECT OF VANADIUM IN B-DOPED FeAl (35.8% Al) CONTAINING 5% Cr .....	19
3.5 EFFECT OF MOLYBDENUM ADDITIONS IN FeAl ALLOYS .....	20
4. CREEP PROPERTIES OF FeAl (35.8% Al) ALLOYS .....	23
5. OXIDATION PROPERTIES .....	25
6. PREPARATION, FABRICATION, AND EVALUATION OF LARGE FeAl ALLOY HEATS .....	25
6.1 MELTING OF FeAl ALLOYS .....	25
6.2 PROCESSING OF FeAl ALLOYS .....	31
6.2.1 Hot Forging .....	35
6.2.2 Hot Extrusion .....	35
6.2.3 Hot Rolling .....	42
6.3 TENSILE TESTING .....	45
7. SUMMARY AND CONCLUSIONS .....	46
8. ACKNOWLEDGMENTS .....	56
9. REFERENCES .....	56

## LIST OF FIGURES

<u>Figure</u>		
		Page
1 Plot of yield strength as a function of aluminum concentration for FeAl alloys tested at temperatures to 700°C .....	5	
2 Plot of tensile elongation as a function of aluminum concentration for FeAl alloys tested at temperatures to 700°C .....	5	
3 SEM fractograph of: (a) FA-318 (36.5% Al) and (b) FA-320 (40% Al) fractured at room temperature .....	6	
4 Twenty-four-hour weight losses of FeAl as a function of aluminum concentration for exposures to $\text{NaNO}_3\text{-KNO}_3\text{-1 mol \% Na}_2\text{O}_2$ at 650°C (ref. 12).....	7	
5 Weight gain as a function of time for FeAl alloys exposed to a gas mixture at 800°C with $\text{PS}_2 = 10^{-6}$ atm and $\text{PO}_2 = 10^{-22}$ atm (ref. 5) .....	8	
6 Electron microprobe analysis of precipitates observed in Fe-35.8Al-0.1Zr-0.12B (at. %): (a) line-scanning of zirconium distribution and (b) line-scanning of boron distribution .....	14	
7 Comparison of grain structure of FeAl (35.8% Al) fabricated by: (a) hot rolling and (b) hot fabrication, 100x .....	16	
8 FA-369 (Fe-35.8Al-0.1Zr-0.24B-5Cr, at. %) produced by hot extrusion at 900°C and annealed for 1 h at 900°C, 100x.....	19	
9 Microstructure of FA-362 (Fe-35.8Al-0.05Zr-0.24B-0.2Mn, at. %) annealed for 1 h at 800 plus 1 h at 700°C: (a) optical micrograph, 200x, and (b) back-scattered electron photograph, 780x .....	22	
10 Plot of weight change as a function of exposure time for FeAl alloys exposed to air at 800°C.....	26	
11 Plot of weight change as a function of exposure time for FeAl alloys exposed to air at 1000°C .....	27	
12 Photograph showing 7.5-kg (15-lb) ingots of FeAl alloys (FA-328, -350, and -362) melted and cast at ORNL. Ingots were melted by air- and vacuum-induction melting in a $\text{ZrO}_2$ crucible. Note the good surface quality .....	29	
13 Photograph showing ingots from 40-kg (80-lb) heats of FeAl alloys (FA-328 and -350) melted at Haynes International. The alloys were vacuum-induction melted, followed by electroslag remelting. Note the excellent surface quality.....	30	

<u>Figure</u>	<u>Page</u>
14 Photograph showing a section of an ingot cast from a 250-kg (500-lb) heat of FeAl alloy (FA-328) melted at The Timken Company. The alloy was air-induction melted and cast into a 200-mm (8-in.)-square ingot. Note the large porosity in the ingot .....	32
15 Photograph showing a section of an ingot cast from a 50-kg (100-lb) heat of FeAl alloy (FA-328) melted at The Timken Company. The alloy was prepared by VIM and cast into a 100-mm-diam tapered ingot. Note the absence of any porosity compared to that observed in air melting .....	33
16 Photograph showing specimen prior to and after hot compressing over 85% in height at temperatures of 800, 900, 1000, and 1100°C. The specimens and the dies were both heated to the same temperature. The compression tests were performed at ORNL .....	35
17 Optical microstructure of hot-extruded bar of FA-350. The ingot was prepared by VIM at ORNL and extruded in a steel wrap at 930°C to an area reduction ratio of 12 to 1: (a) shows the bar edge, (b) one-half radius, and (c) bar center locations for a transverse section .....	37
18 Optical microstructure of hot-extruded rectangular bar of FA-362. The ingot was prepared by VIM at ORNL and extruded in a steel wrap at 1000°C to a reduction ratio of 4 to 1: (a) shows the bar edge, (b) mid thickness, and (c) other edge of longitudinal section, and (d), (e), and (f) show the same locations for the transverse section .....	38
19 Optical microstructure of hot-extruded bar of FA-350. The ingot was prepared by VIM at The Timken Company and extruded in a steel can in two steps to a 25-mm-diam bar. The area reduction ratios for steps 1 and 2 were 3.35 and 9 to 1, respectively: (a) shows the bar edge, (b) one-half radius, and (c) bar center locations .....	39
20 Optical microstructure of hot-extruded bar of FA-350. The ingot was prepared by VIM at ORNL and extruded in a steel wrap at 1000°C to an area reduction ratio of 9 to 1: (a) shows the bar edge, (b) one-half radius, and (c) bar center locations for the longitudinal section, and (d), (e), and (f) show the same locations for the transverse section .....	40
21 Comparison of high-magnification micrographs of 25-mm-diam bars of FeAl alloy FA-350: (a) and (b) are transverse sections of Timken- and ORNL-melted materials .....	41
22 Photograph showing the tubing of FA-362 in the as-extruded condition and a piece of it after acid cleaning. The tube was extruded in a steel wrap at 1100°C from air-induction-melted ingot at ORNL .....	42

<u>Figure</u>	<u>Page</u>
23 Optical microstructure of the tubing of FA-362 in the as-extruded condition: (a) shows OD, (b) mid thickness, and (c) ID locations of longitudinal cross section of the tube, and (d), (e), and (f) are OD, mid thickness, and ID locations, respectively, of transverse cross section of the tube .....	43
24 Optical microstructure of the 0.76-mm-thick sheet of FA-362 in the as-rolled condition: (a) and (b) are the longitudinal and transverse directions of the sheet.....	44
25 Plot of yield and ultimate tensile strength as a function of test temperature for sheet specimens of FA-350. The sheet was stress relieved at 700°C for 1 h, followed by oil quenching prior to punching specimens. The specimens were given an annealing treatment at 700°C for 1 h, followed by oil quenching prior to tensile testing. All of the tests were in air at a strain rate of 0.2/min ( $3.33 \times 10^{-3}/s$ ) .....	48
26 Plot of total elongation and reduction of area as a function of test temperature for sheet specimens of FA-350. The sheet was stress relieved at 700°C for 1 h, followed by oil quenching prior to punching specimens. The specimens were given an annealing treatment at 700°C for 1 h, followed by oil quenching prior to tensile testing. All of the tests were in air at a strain rate of 0.2/min ( $3.33 \times 10^{-3}/s$ ) .....	49
27 Plot of yield and ultimate tensile strength as a function of test temperature for sheet specimens of FA-362. The sheet was stress relieved at 700°C for 1 h, followed by oil quenching prior to punching specimens. The specimens were given an annealing treatment at 700°C for 1 h, followed by oil quenching prior to tensile testing. All of the tests were in air at a strain rate of 0.2/min ( $3.33 \times 10^{-3}/s$ ) .....	50
28 Plot of total elongation and reduction of area as a function of test temperature for sheet specimens of FeAl alloy FA-362. The sheet was stress relieved at 700°C for 1 h, followed by oil quenching prior to punching specimens. The specimens were given an annealing treatment at 700°C for 1 h, followed by oil quenching prior to tensile testing. All of the tests were in air at a strain rate of 0.2/min ( $3.33 \times 10^{-3}/s$ ) .....	51
29 Comparison of yield strength of FA-350 and -362 in sheet form as a function of test temperature .....	52
30 Comparison of ultimate tensile strength of FA-350 and -362 in sheet form as a function of test temperature .....	52
31 Comparison of total elongation of FA-350 and -362 in sheet form as a function of test temperature .....	53
32 Comparison of reduction of area of FA-350 and -362 in sheet form as a function of test temperature .....	53

## LIST OF TABLES

<u>Table</u>		
	<u>Page</u>	
1 Composition of binary FeAl alloys.....	3	
2 Creep properties of FeAl alloys tested at 207 MPa (30 ksi) and 593°C (1100°F).....	7	
3 Effect of chromium on tensile properties of Fe-35.8 at. % Al .....	10	
4 Effect of boron additions on room-temperature tensile properties of Fe-35.8% Al .....	10	
5 Effect of zirconium additions on properties of Fe-35.8% Al.....	11	
6 Effect of boron and zirconium additions on tensile properties of FeAl (35.8% Al).....	13	
7 Tensile properties of FeAl (35.8% Al) alloys produced by hot rolling (sheet material) or hot extrusion (rod material).....	15	
8 Effect of surface treatment on room-temperature tensile properties of FA-350 (Fe-35.8Al-0.05Zr-0.24B, at. %).....	18	
9 Effect of chromium additions on tensile properties of FA-342-type alloys.....	18	
10 Effect of 0.5% V on tensile properties of B-doped FeAl (35.8% Al) containing 5% Cr .....	20	
11 Effect of molybdenum additions on tensile properties of FeAl (35.8% Al) alloys.....	21	
12 Electron microprobe analyses of chemical composition of FA-362, -363, and -364 alloys .....	23	
13 Creep properties of FeAl (35.8% Al) alloys tested at 138 MPa (20 ksi) and 593°C (1100°F).....	24	
14 Chemical analysis of alloy FA-350 prepared by electroslag remelting at Haynes International .....	31	
15 Target and check analysis of alloy FA-350 vacuum-induction melted at The Timken Company .....	34	

<u>Table</u>	<u>Page</u>
16 Tensile properties of hot-extruded bar of FA-350 iron-aluminide alloy. The alloy was prepared by VIM and cast into 72-mm (2.85-in.)-diam ingots. The ingots were hot extruded in a steel wrap at 930 and 1000°C to an area reduction ratio of 12 to 1. Specimens were given an annealing treatment at 700°C for 1 h followed by oil quenching. Data on the bar extruded at 1000°C, forged at 1000°C, and hot rolled into sheet at 800°C are also included for comparison. All of the tests were done in air at a strain rate of $3.33 \times 10^{-3}/s$ .....	45
17 Tensile properties of 0.76-mm steel specimens of 7.5-kg (15-lb) heat of FA-350 alloy. The heat was vacuum-induction melted and cast into a 72-mm-diam ingot. The ingot was extruded at 1000°C in a mild steel wrap into a 25-mm-diam bar. The bar was forged flat at 1000°C and hot rolled in a steel cover at 800°C to a thickness of 0.76 mm. The sheet was stress relieved at 700°C for 1 h, followed by oil quenching. The punched specimens were annealed for 1 h at 700°C, followed by oil quenching.....	47
18. Tensile properties on 0.76-mm sheet specimens of 7.5-kg (15-lb) heat (13998) of FA-362 alloy. The heat was melted by the <u>air-induction-melted</u> process and cast into a 72-mm-diam ingot. The ingot was extruded at 1000°C in a mild steel wrap into a rectangular cross section. The extruded cross section was hot rolled in a steel cover at 900°C to 0.76-mm-thick sheet. The sheet was stress relieved at 700°C for 1 h, followed by oil quenching. The punched specimens were annealed for 1 h at 700°C, followed by oil quenching.....	47

## ALLOY DEVELOPMENT OF FeAl ALUMINIDE ALLOYS FOR STRUCTURAL USE IN CORROSIVE ENVIRONMENTS\*

C. T. Liu, V. K. Sikka, and C. G. McKamey

### ABSTRACT

This is an interim report on the project to develop an iron aluminide alloy for structural use in corrosive environments. Specific target objectives of the aluminide alloys include adequate ductilities ( $\geq 10\%$ ) at ambient temperature, high-temperature strength better than stainless steels (types 304 and 316), and fabricability and weldability by conventional techniques (gas tungsten arc). The alloys should be capable of being corrosion resistant in molten nitrate salt environments with rates lower than iron-base structural alloys and coating materials (such as Fe-Cr-Al alloys) that are currently available commercially. For oxidizing molten nitrate salt environments, such corrosion rates should be less than 0.3 mm per year. The FeAl aluminide containing 35.8 at. % Al was selected as the base composition for alloy development. Preliminary alloying studies indicate that additions of B and Zr, either individually or synergistically, effectively increase the room-temperature ductility of FeAl. Further alloying with 0.2% Mo, with or without 5% Cr, improves the creep properties of FeAl alloys. Our preliminary alloying effort has led to identification of the following aluminide composition with promising properties:

Fe -  $(35 \pm 2)$ Al -  $(0.3 \pm 0.2)$ Mo -  $(0.2 \pm 0.15)$ Zr -  $(0.3 \pm 0.2)$ B- up to 5Cr, at. %.

However, this composition is likely to be modified in future work to improve the weldability of the alloy. The FeAl alloy FA-362 (Fe-35.8% Al-0.2% Mo-0.05% Zr-0.24% B) produced by hot extrusion at 900°C showed a tensile ductility of more than 10% at room temperature and a creep rupture life longer than unalloyed FeAl by more than an order of magnitude at 593°C (1100°F) at 138 MPa.

The melting and processing of scaled-up heats of selected FeAl alloys are described. Scale-up heats of 7.5, 40, and 250 kg (15, 80, and 500 lb) were melted at Oak Ridge National Laboratory (ORNL), Haynes International, and the Timken Company. Forging, extruding, and hot-rolling processes for the scale-up heats are also described along with their microstructures and mechanical properties.

---

\*Research sponsored by the U.S. Department of Energy, Assistant Secretary for Conservation and Renewable Energy, Office of Industrial Technologies, Advanced Industrial Concepts (AIC) Materials Program, under contract DE-AC05-84OR21400 with Martin Marietta Energy Systems, Inc.

## 1. INTRODUCTION

The objective of this research is to develop a low-cost, low-density, fabricable, corrosion-resistant FeAl aluminide that will have broad applications in energy-efficient processes and systems. Specific target objectives of the aluminide alloys include adequate ductilities ( $\geq 10\%$ ) at ambient temperature, high-temperature strength better than stainless steels (types 304 and 316), and fabricability and weldability by conventional techniques (gas tungsten arc). The iron aluminide forms a body-centered cubic (bcc)-ordered crystal structure, B2, over the composition range of 30 to 51 at. % Al (ref. 1). The aluminide possesses unique properties and has the potential to be developed as new structural materials for use in hostile environments at temperatures to 700°C. This is because FeAl is capable of forming protective aluminum oxide scales at very low-oxygen partial pressures at elevated temperatures.<sup>2-5</sup> In addition to corrosion resistance, the aluminide also offers relatively low material cost, low density ( $\rho = 5.6$  g/cc), and conservation of strategic elements (such as Cr and Co), all of which provide economic benefits very important to U.S. industries.

Structural use of binary iron aluminides has been limited by their low ductility and fracture toughness at ambient temperatures, and a sharp drop in strength above 600°C. Previous studies of Fe<sub>3</sub>Al and FeAl aluminides indicated a general trend: as the aluminum content is increased, the aluminide alloys exhibit better corrosion resistance but become less ductile and more difficult to fabricate.<sup>2-10</sup> In some cases, a critical level of aluminum is required in order to achieve corrosion rates acceptable for industrial applications.<sup>11-13</sup> The initial development work in this project has thus focused on improving room-temperature ductility and high-temperature strength (including creep properties) without sacrificing the excellent corrosion resistance of FeAl. Emphasis has been placed on development of a new corrosion-resistant structural alloy for molten salt systems for chemical air separation.<sup>11-13</sup> In this case, the structural material is required to have corrosion rates lower than 0.3 mm per year when exposed to molten sodium-potassium nitrate salts at temperatures to 650°C.

The development of FeAl for structural use in corrosive environments is jointly sponsored by the Department of Energy (DOE) Advanced Industrial Materials (AIM) Program and Office of Industrial Technologies (OIT). The development work includes the following subtasks: (1) selection of a base binary composition of FeAl for alloying studies, (2) improvement of metallurgical and mechanical properties of FeAl by control of microstructure and alloy additions, (3) preparation and evaluation of large heats with optimum compositions, and (4) evaluation of corrosion properties of FeAl alloys exposed

to molten salt environments at elevated temperatures. This report summarizes the results obtained from the first three subtasks; those from the fourth subtask were reported separately by Tortorelli and Bishop.<sup>12</sup> Some weldability work has been conducted but will not be described in this report.

## 2. STUDY OF BINARY FeAl ALLOYS

Mechanical properties of FeAl are known to be dependent on the aluminum level.<sup>2-10</sup> The first phase of this development is to determine an optimum level of aluminum in FeAl for alloying studies. Early results from corrosion studies with highly oxidizing molten nitrate salts demonstrated that FeAl had superior corrosion resistance relative to many other metals and alloys and indicated the necessity of an aluminum concentration of greater than 30 at. % (ref. 11). Several alloy ingots containing 30 to 43 at. % Al (see Table 1), weighing 400 g each, were prepared by arc melting and drop casting. All the alloys were clad in steel plates and successfully fabricated into 0.76-mm-thick sheets by hot rolling at temperatures of 1100 to 900°C. Tensile and creep specimens prepared from sheet stock were given a standard heat treatment of 1 h at 900°C for complete recrystallization and 2 h at 700°C for ordering into the B2 structure. All the alloys showed a coarse grain structure, with a grain size of ~200 µm.

Table 1. Composition of binary FeAl alloys

Alloy number	Nominal composition (at. % Al)
FA-315	30.0
FA-316	32.5
FA-317	35.0
FA-318	36.5
FA-319	38.0
FA-320	40.0
FA-321	43.0

Tensile properties of binary FeAl alloys were determined as a function of temperature (to 700°C) in air. Figure 1 shows a plot of the yield strength of FeAl alloys as a function of aluminum concentration. The alloys show a general increase in yield strength with aluminum at temperatures to 400°C. The strength becomes insensitive to the aluminum concentration at 600°C, and it shows a general decrease with aluminum at 700°C. Note that a drop in yield strength of the 43 at. % Al alloy tested at room and elevated temperatures is due to fracture prior to macroscopic yielding. Figure 2 is a plot of tensile elongation as a function of aluminum concentration. At temperatures to 400°C, the elongation shows a general trend of decreasing with the aluminum level. At higher temperatures, the alloys exhibit a peak ductility around 35 to 38% Al.

Scanning electron microscopy (SEM) examinations of specimens fractured at room temperature reveal that the alloys with less than 38 at. % Al fractured mainly by transgranular cleavage while the alloys with more than 38% Al failed essentially by grain-boundary separation (see Fig. 3). In the past, the low ductility and brittle cleavage fracture in  $\text{Fe}_3\text{Al}$  and FeAl were mainly attributed to their poor cohesive strength across certain crystallographic planes.<sup>14-18</sup> However, recent studies have demonstrated that the iron aluminides are intrinsically quite ductile and that poor ductility and brittle cleavage fracture are caused by environmental embrittlement when tested in air at ambient temperatures.<sup>19-21</sup> The embrittlement involves the reaction of aluminum atoms in the alloys with moisture in air, resulting in generation of atomic hydrogen that drives into crack tips and causes premature failure along cleavage planes.

Creep properties of FeAl alloys were characterized by testing at 593°C (1200°F) and 207 MPa (30 ksi) in air. The results are summarized in Table 2. In general, the creep resistance shows a slight decrease with increasing aluminum concentration; however, all alloys ruptured within 5 h. For comparison, type 316 stainless steel ruptured in about 100 h at the same test conditions. Thus, the binary FeAl alloys are weak in creep, and alloy development is required to improve their creep properties. Table 2 also shows that the creep-rupture elongation varies from 10 to 35% when tested in creep at 593°C.

The corrosion studies by Tortorelli and Bishop<sup>12-13</sup> revealed that the corrosion resistance of FeAl in molten nitrate-peroxide salts did not dramatically change as a function of aluminum concentration once a minimum of 30% was achieved (see Fig. 4). Furthermore, DeVan showed that binary FeAl had excellent resistance to oxidation/sulfidation even at low-oxygen partial pressure (see Fig. 5, ref. 5). Therefore, based on tensile properties, hot fabricability, creep properties, and corrosion resistance, the FeAl alloy containing 35.8% Al was selected as the base binary composition for future alloying studies.

ORNL-DWG 92-11975

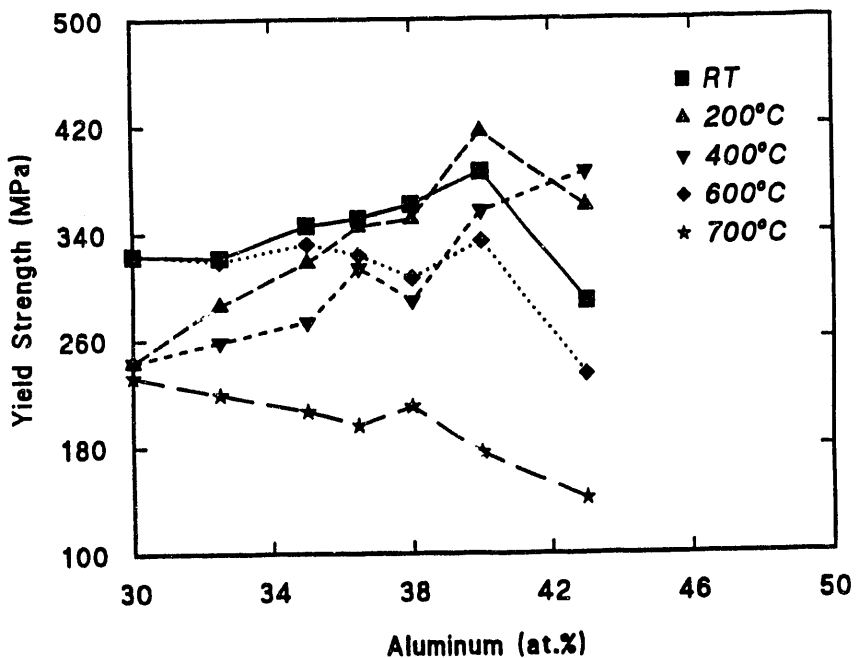


Fig. 1. Plot of yield strength as a function of aluminum concentration for FeAl alloys tested at temperatures to 700°C.

ORNL-DWG 92-11976

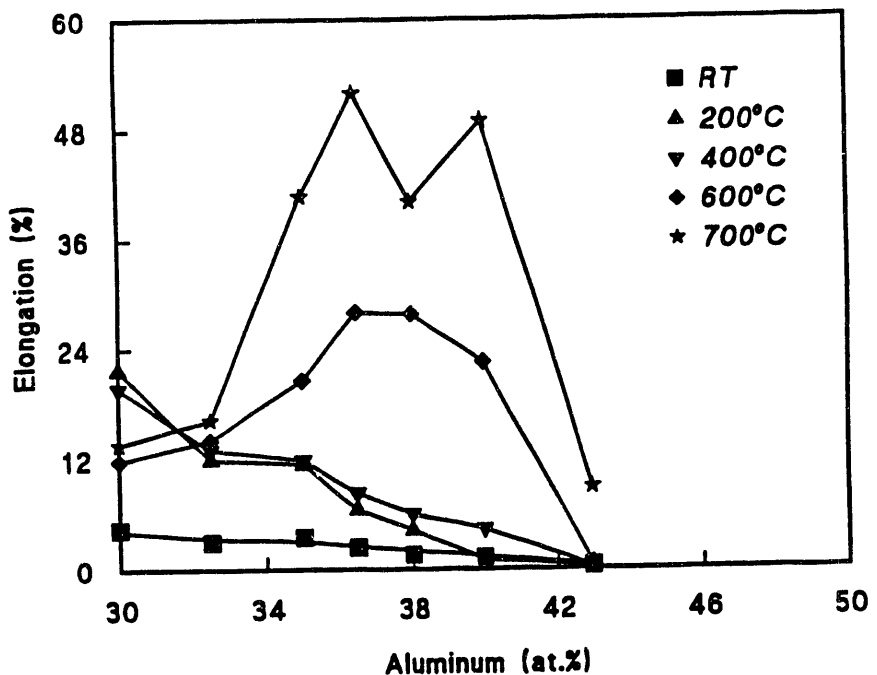


Fig. 2. Plot of tensile elongation as a function of aluminum concentration for FeAl alloys tested at temperatures to 700°C.

M29272

(a)



15KV X100 9272 100.00 M&amp;C

M29287

(b)



15KV X100 9287 100.00 M&amp;C

Fig. 3. SEM fractograph of: (a) FA-318 (36.5% Al) and (b) FA-320 (40% Al) fractured at room temperature.

Table 2. Creep properties of FeAl alloys tested at 207 MPa (30 ksi) and 593°C (1100°F)

Alloy number	Al %	Rupture life (h)	Rupture elongation (%)
FA-315	30.0	2.6	10.5
FA-316	32.5	4.5	11.0
FA-317	35.0	2.0	19.6
FA-318	36.5	1.8	19.1
FA-319	38.0	0.8	25.5
FA-320	40.0	0.6	35.4
FA-321	43.0	0.2	22.0

ORNL-DWG 92-11977

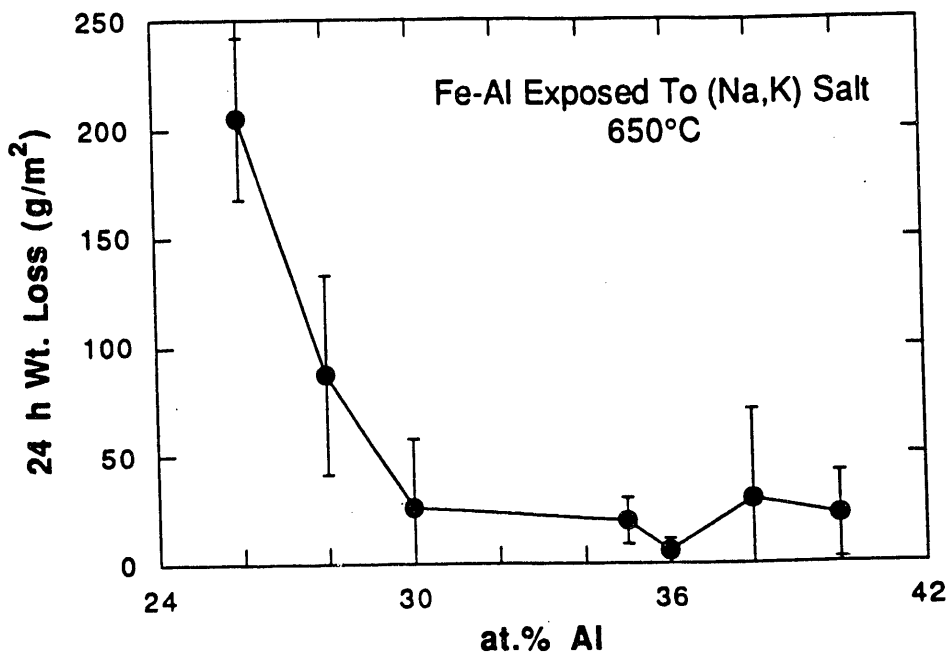


Fig. 4. Twenty-four-hour weight losses of FeAl as a function of aluminum concentration for exposures to  $\text{NaNO}_3\text{-KNO}_3\text{-1 mol \% Na}_2\text{O}_2$  at 650°C (ref. 12.).

ORNL-DWG 92-11978

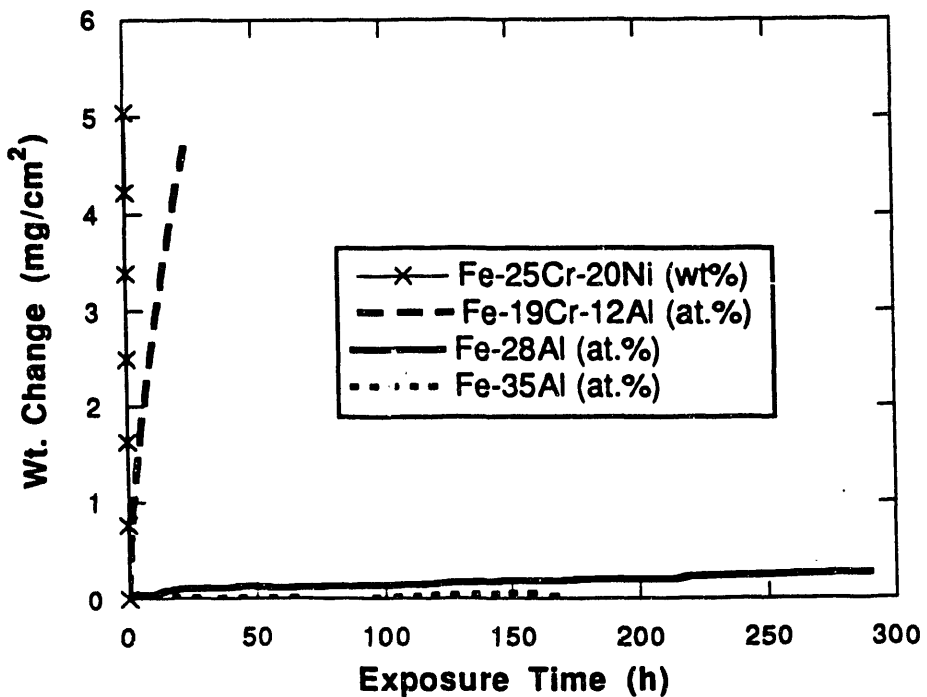


Fig. 5. Weight gain as a function of time for FeAl alloys exposed to a gas mixture at 800°C with  $PS_2 = 10^{-6}$  atm and  $PO_2 = 10^{-22}$  atm (ref. 5).

### 3. EFFECT OF ALLOY ADDITIONS ON STRUCTURE AND PROPERTIES OF Fe-35.8% Al

This phase of alloy development has focused on improving the metallurgical and mechanical properties of FeAl containing 35.8 at. % Al by alloy additions. Our initial effort was devoted mainly to improving the tensile elongation at ambient temperatures. The binary aluminide showed brittle cleavage fracture and a low ductility of 2.2% at room temperature because of environmental embrittlement due to moisture in air.<sup>19-21</sup> The improvement in ductility required controlling the surface composition and microstructure of FeAl alloys.

Based on consideration of surface reaction and environmental embrittlement, a group of alloying elements was selected and added at levels up to 10 at. % to FeAl containing 35.8% Al. The elements added included Cr, Ni, Co, Mn, Ti, Zr, V, Mo, B, and C.

Among these elements, we found that adding Ni, Co, Mn, Ti, and C did not produce any significant improvement in properties, and these results are not discussed in detail in this report.

### 3.1 Cr EFFECT

Chromium was reported to improve tensile properties of  $\text{Fe}_3\text{Al}$  alloys<sup>17,18,22</sup> and thus was selected for addition to Fe-35.8 at. % Al. FeAl alloys containing up to 5 at. % Cr were prepared by arc melting and drop casting, followed by hot fabrication similar to the binary alloys. In general, chromium additions do not effect hot fabricability of Fe-35.8% Al.

Tensile properties of chromium-modified FeAl alloys are tabulated in Table 3. Chromium additions slightly lower the yield strength of FeAl but do not improve the room-temperature ductility. Alloying with 5 at. % Cr causes a slight decrease in ductility at room temperature and 200°C, and a significant decrease at 600°C. This result is apparently different from what was obtained in the case of  $\text{Fe}_3\text{Al}$  (28% Al), which showed an increase in room-temperature tensile elongation from 4 to 8 to 10% when alloyed with 2 to 6% Cr (refs. 17,18).

### 3.2 B AND Zr EFFECTS

Boron at levels to 0.6 at. % (1500 wt ppm) was added to FeAl (35.8 at. % Al) prepared by arc melting and drop casting (see Table 4). Surprisingly, alloying with as little as 150 wt ppm B (0.06 at. %) causes several edge and end cracks during hot rolling at 1100 to 1000°C. Thus, only limited sheet materials were available for property evaluation. The hot cracking is presumably related to incipient melting induced by boron additions to FeAl.

Table 4 shows the effect of boron additions on room-temperature tensile properties of Fe-35.8% Al tested in air. The yield strength appears to decrease with boron addition, and ultimate tensile strength changes with ductility. Boron significantly increases the tensile elongation with a maximum ductility located around 0.12% B (300 ppm). Additional boron causes a small decrease in ductility.

In contrast to boron, zirconium additions were found to have no adverse effect on sheet fabrication during hot rolling. Table 5 summarizes the tensile properties of FeAl alloys containing zirconium additions. Binary FeAl showed a decrease in yield strength with temperature, followed by an increase. The minimum strength is located around 400°C. The alloy exhibited a general increase in ductility with temperature, although it

Table 3. Effect of chromium on tensile properties of Fe-35.8 at. % Al

Cr level (at. %)	Elongation (%)	Yield strength, MPa (ksi)	Tensile strength, MPa (ksi)
<b>Room temperature</b>			
0	2.2	355 (51.5)	409 (59.4)
2	2.5	329 (47.8)	383 (55.6)
5	1.9	306 (44.4)	342 (49.6)
<b>200°C</b>			
0	9.0	312 (45.9)	576 (83.6)
2	8.3	319 (46.3)	547 (79.4)
5	7.8	298 (43.3)	508 (73.8)
<b>600°C</b>			
0	20.1	332 (48.2)	394 (57.2)
2	10.6	316 (45.8)	403 (58.5)
5	6.2	299 (43.4)	406 (58.9)

Table 4. Effect of boron additions on room-temperature tensile properties of Fe-35.8% Al

Alloy number	B concentration (wt ppm)	Strength, MPa (ksi)		Elongation (%)
		Yield	Tensile	
FA-324	0	355 (51.5)	409 (59.4)	2.2
FA-337	150	318 (46.1)	392 (56.9)	3.0
FA-325	300	358 (52.0)	567 (82.4)	5.6
FA-338	600	315 (45.7)	440 (63.9)	3.5
FA-339	1000	308 (44.7)	389 (56.5)	3.1
FA-340	1500	282 (41.0)	368 (53.4)	3.3

Table 5. Effect of zirconium additions on properties of Fe-35.8% Al

Alloy number	Zr concentration (at. %)	Strength, MPa (ksi)		Elongation (%)
		Yield	Tensile	
<b>Room temperature</b>				
FA-324	0	355 (51.5)	409 (59.4)	2.2
FA-326	0.1	282 (41.0)	425 (61.7)	4.6
FA-346	0.2	291 (42.3)	464 (67.3)	4.6
FA-347	0.4	307 (44.6)	460 (66.8)	3.8
FA-348	0.6	331 (48.1)	494 (71.7)	3.8
FA-349	1.0	380 (55.2)	569 (82.6)	3.8
<b>200°C</b>				
FA-324	0	316 (45.9)	576 (83.6)	9.0
FA-326	0.1	262 (38.0)	610 (88.5)	10.8
FA-346	0.2	269 (39.0)	588 (85.3)	7.8
FA-347	0.4	251 (36.4)	582 (84.4)	8.3
FA-348	0.6	287 (41.7)	672 (97.5)	9.3
FA-349	1.0	342 (49.6)	699 (101.5)	8.2
<b>400°C</b>				
FA-324	0	294 (42.6)	450 (65.3)	7.4
FA-326	0.1	274 (39.8)	513 (74.4)	8.9
FA-346	0.2	269 (39.0)	591 (85.8)	12.2
FA-347	0.4	--	--	--
FA-348	0.6	325 (47.2)	626 (90.8)	9.0
FA-349	1.0	348 (50.5)	630 (91.5)	6.7
<b>600°C</b>				
FA-324	0	332 (48.2)	394 (57.2)	20.1
FA-326	0.1	309 (44.8)	411 (59.6)	22.9
FA-346	0.2	306 (44.4)	412 (59.8)	25.4
FA-347	0.4	316 (45.9)	440 (63.9)	27.3
FA-348	0.6	315 (45.7)	454 (65.9)	19.6
FA-349	1.0	328 (47.6)	496 (72.0)	19.2

showed no major change in ductility at 200 to 400°C. The increase in yield strength with temperature above 200 to 400°C has been observed in other FeAl and Fe<sub>3</sub>Al alloys.<sup>6-9,23</sup>

Alloying with 0.1 at. % Zr results in a moderate decrease in yield strength and an increase in tensile ductility at room and elevated temperatures (see Table 5). The yield strength is insensitive to zirconium at 0.1 to 0.4% and increases significantly above 0.4% Zr. The ductility appears to peak around 0.1 to 0.2% Zr at room temperature and is not significantly affected by zirconium additions at elevated temperatures.

Since both boron and zirconium are beneficial to the room-temperature ductility of FeAl, a combination of 0.1% Zr with different levels of boron was added to Fe-35.8% Al (see Table 6). All the alloys have good hot fabricability with end cracks observed only in the alloy containing 0.4 and 0.6 at. % B. All specimens punched from sheet stock were annealed 1 h at 900°C + 2 h at 700°C for tensile property evaluation.

Table 6 summarizes tensile properties at temperatures to 700°C. As indicated in Tables 4 and 5, the optimum amounts of boron and zirconium for room-temperature ductility improvement in FeAl are 0.12 and 0.1%, respectively. Surprisingly, a simple combination of 0.12% B and 0.1% Zr (FA-341) did not give the expected beneficial effect in Fe-35.8% Al. It appears that the boron-to-zirconium atom ratio plays an important role in improving the room-temperature ductility. As indicated in Table 6, the benefit of a combined effect of zirconium and boron is detected when the B/Zr ratio is larger than two. The alloys FA-351 and -352 containing the highest levels of boron show the best ductilities at 600 and 700°C. Alloying with 0.1% Zr + B lowers yield strength at room temperature and 200°C, does not affect the strength at 400 and 600°C, and increases the strength at 700°C. The best strength at 700°C is obtained in the alloy FA-342 containing 0.24% B and 0.1% Zr.

The phases present in FA-341 and -342 were studied by electron microprobe analysis. Fine, second-phase particles are observed in these alloys as shown in Fig. 6(a). Line-scanning indicates enrichment of zirconium and boron in these particles [see Fig. 6(b)], presumably ZrB<sub>2</sub> particles. This result confirms the importance of the B/Zr ratio. With the ratio >2, boron is available in solid solution and may contribute to improvement in room-temperature ductility of FeAl alloy. Table 6 indicates that the ductility is not sensitive to the amount of boron in solid solution as long as the ratio of B/Zr is larger than two.

The hot-rolling procedure used here produced sheet materials with a rather coarse grain structure (grain diameter  $\approx$ 200  $\mu$ m). To evaluate the grain-size effect, a number of alloy ingots were fabricated by hot extrusion at 900°C with an extrusion ratio of 12 to 1.

Table 6. Effect of boron and zirconium additions on tensile properties of FeAl (35.8% Al)

Alloy number	(Zr + B) concentration (at. %)	Strength, MPa (ksi)		Elongation (%)
		Yield	Tensile	
<b>Room temperature</b>				
FA-324	0	355 (51.5)	409 (59.4)	2.2
FA-341	0.1Zr + 0.12B	290 (42.1)	358 (51.9)	2.6
FA-342	0.1Zr + 0.24B	320 (46.5)	489 (71.0)	4.8
FA-351	0.1Zr + 0.40B	298 (43.2)	491 (71.3)	4.8
FA-352	0.1Zr + 0.60B	310 (45.0)	483 (70.1)	4.8
<b>200 °C</b>				
FA-324	0	316 (45.9)	576 (83.6)	9.0
FA-341	0.1Zr + 0.12B	269 (39.1)	476 (69.1)	6.5
FA-342	0.1Zr + 0.24B	295 (42.8)	599 (87.0)	9.6
FA-351	0.1Zr + 0.40B	285 (41.4)	652 (94.6)	12.0
FA-352	0.1Zr + 0.60B	290 (42.1)	634 (92.0)	9.6
<b>400 °C</b>				
FA-324	0	294 (42.6)	450 (65.3)	7.4
FA-341	0.1Zr + 0.12B	263 (38.1)	473 (68.6)	7.4
FA-342	0.1Zr + 0.24B	294 (42.7)	532 (77.2)	8.4
FA-351	0.1Zr + 0.40B	295 (42.8)	553 (80.3)	9.2
FA-352	0.1Zr + 0.60B	269 (39.0)	511 (74.1)	7.7
<b>600 °C</b>				
FA-324	0	332 (48.2)	394 (57.2)	20.1
FA-341	0.1Zr + 0.12B	305 (44.3)	407 (59.1)	13.8
FA-342	0.1Zr + 0.24B	303 (44.0)	449 (65.2)	20.3
FA-351	0.1Zr + 0.40B	316 (45.8)	370 (53.7)	87.5
FA-352	0.1Zr + 0.60B	321 (46.6)	407 (59.0)	35.4
<b>700 °C</b>				
FA-324	0	212 (30.8)	218 (31.6)	24.4
FA-341	0.1Zr + 0.12B	252 (36.5)	280 (40.7)	37.4
FA-342	0.1Zr + 0.24B	271 (39.4)	292 (42.4)	42.7
FA-351	0.1Zr + 0.40B	—	—	—
FA-352	0.1Zr + 0.60B	228 (33.1)	258 (37.5)	48.6

ORNL/DWG 93-5797

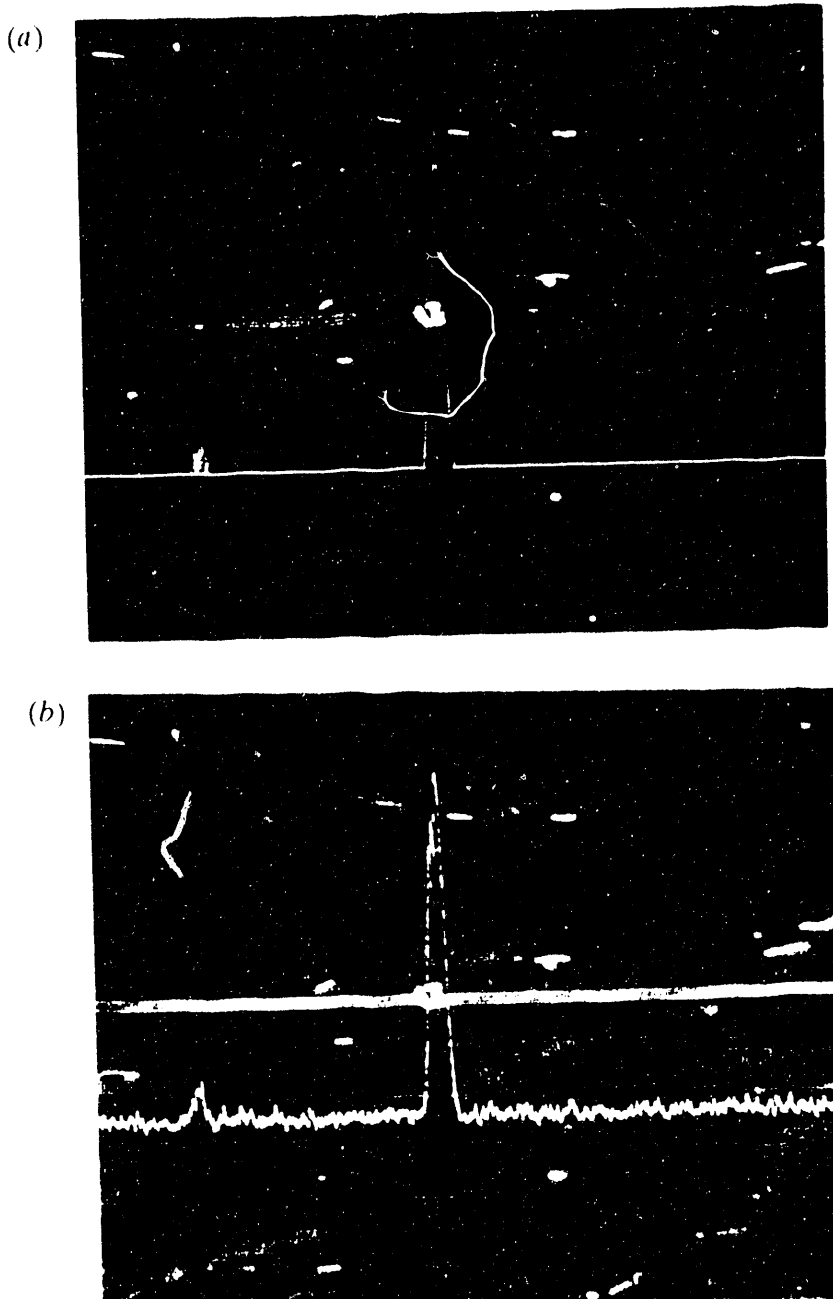


Fig. 6. Electron microprobe analysis of precipitates observed in Fe-35.8Al-0.1Zr-0.12B (at. %): (a) line-scanning of zirconium distribution and (b) line-scanning of boron distribution.

All alloys in Table 7 were successfully extruded into bar stock without difficulty. As shown in Fig. 7 for FeAl (35.8% Al), the hot-extruded rod material had a grain size smaller than that of hot-rolled sheet material by a factor of about seven.

Table 7 compares the tensile properties of three FeAl alloys with different grain sizes. All tensile specimens (3.12 mm diam by 17.8 mm long) were annealed for 1 h at 600 to 700°C after the extrusion. The hot-extruded materials with a fine grain structure are much more ductile at room temperature and 600°C than hot-rolled material with a coarse grain structure. A room-temperature elongation of 10.7% is achieved by FA-350 (Fe-35.8Al-0.05Zr-0.24B) [B/Zr = 4.8] produced by hot extrusion. As indicated in Table 7, the yield strength is not sensitive to test temperature for both hot-extruded and hot-rolled materials.

Table 7. Tensile properties of FeAl (35.8% Al) alloys produced by hot rolling (sheet material) and hot extrusion (rod material)

Alloy number	Alloy composition	Elongation (%)	Strength, MPa (ksi)	
			Yield	Ultimate
<b>Room temperature, sheet specimens (coarse grain size)</b>				
FA-324	35.8Al	2.2	356 (51.6)	409 (59.4)
FA-342	35.8Al + 0.1Zr + 0.24B	4.7	320 (46.5)	489 (71.0)
FA-350	35.8Al + 0.05Zr + 0.24B	4.5	300 (43.5)	442 (64.1)
<b>Room temperature, rod specimens (fine grain size)</b>				
FA-324		7.6	335 (48.6)	621 (90.2)
FA-342		9.1	337 (48.9)	740 (107.4)
FA-350		10.7	325 (47.2)	755 (109.6)
<b>600°C, sheet specimens (coarse grain size)</b>				
FA-324		20.1	332 (48.2)	394 (57.2)
FA-342		20.3	372 (54.0)	449 (65.2)
FA-350		19.2	332 (48.2)	411 (59.7)
<b>600°C, rod specimens (fine grain size)</b>				
FA-324		49.3	312 (45.3)	353 (51.3)
FA-342		57.4	351 (51.0)	368 (53.4)
FA-350		54.9	360 (52.2)	390 (56.6)

ORNL/DWG 93-5798

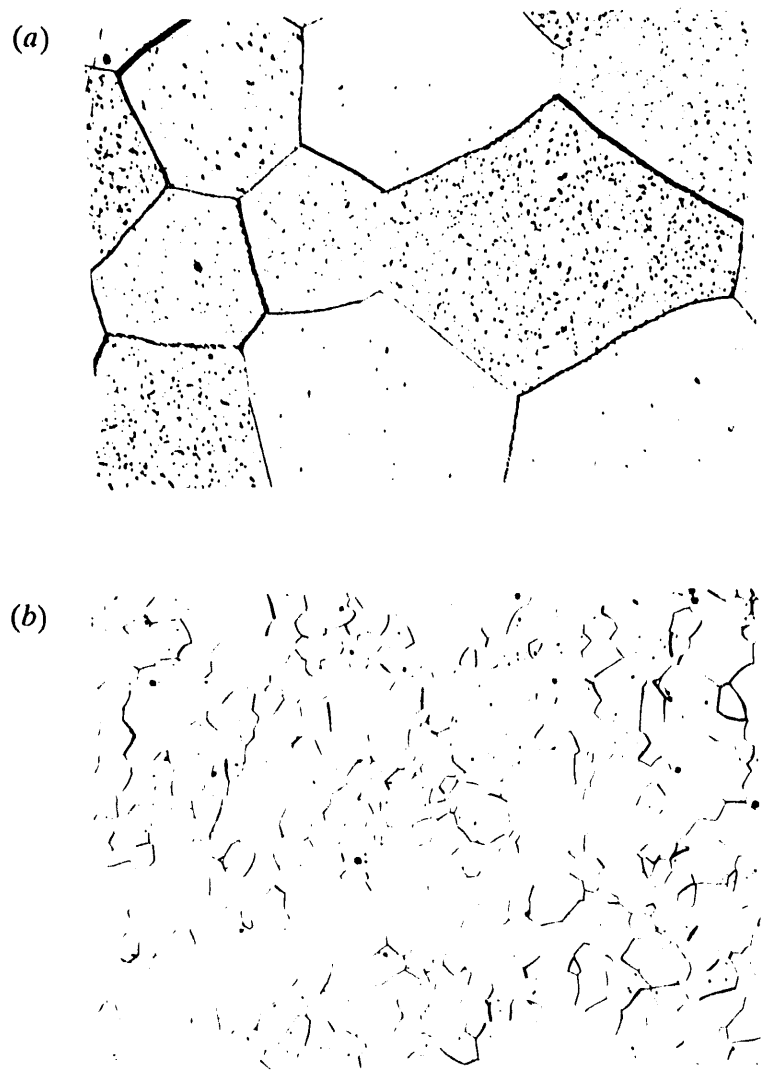


Fig. 7. Comparison of grain structure of FeAl (35.8% Al) fabricated by: (a) hot rolling and (b) hot fabrication, 100 $\times$ .

Since FeAl alloys are susceptible to environmental embrittlement at ambient temperatures,<sup>19-21</sup> it is expected that the surface condition of specimens will affect the ductility. This is illustrated in Table 8 for FA-350 tested at room temperature in air. The bare specimens heat treated for 1 h at 700°C in vacuum (no apparent oxide layer on specimen surfaces) showed 10.7% elongation. Coating the surfaces with oil increases the ductility to 13.4%. The ductility of FA-350 further increased to 14.2% when the bare specimens were annealed six times at 700°C for 30 min each in air, followed by cooling each time to room temperature. The heat treatment of FA-350 in air produced thin oxide scales on the specimen surfaces that apparently reduce the embrittlement by moisture in air during tensile tests. This result demonstrates that the control of surface conditions is effective in reducing environmental embrittlement in FeAl alloys.

FeAl alloys containing  $\geq 40\%$  were reported to fail at room temperature by intergranular fracture with little tensile ductility.<sup>6,7</sup> Small additions of boron (0.05 to 0.2%) suppressed the grain-boundary fracture and allowed a small increase in the ductility (~3%) of Fe-40% Al but not of Fe-50% Al.<sup>24</sup> The beneficial effect was nowhere near as dramatic as in Ni<sub>3</sub>Al, but was nevertheless significant. The ductility of boron-doped FeAl (40% Al) exhibited a high tensile ductility of ~18% when tested in dry oxygen to avoid environmental embrittlement.<sup>21</sup>

### 3.3 Cr EFFECTS IN FA-342 (Fe-35.8Al-0.1Zr-0.24B, at. %) TYPE ALLOYS

As shown above, our studies indicate that a proper combination of B and Zr (i.e., B/Zr  $> 2$ ) increases the room-temperature ductility of FeAl (35.8% Al). Chromium additions were therefore added to FA-342 for possible improvement in alloy properties. Table 9 lists the composition of these alloys, which were prepared by hot extrusion at 900°C at an extrusion ratio of 9 to 1. Chromium was added to replace iron in these alloys. Figure 8 shows the fine grain structure of FA-369 (containing 5% Cr) annealed for 1 h at 900°C. The alloy showed very little grain growth until the annealing temperature reached 1100°C.

Table 9 summarizes the tensile properties of the alloys based on FA-342 containing up to 5 at. % Cr. Tensile specimens were annealed at 700 to 900°C to produce a recrystallized grain structure and then tested in air at room temperature and 600°C. The yield strength appears to decrease slightly with chromium at these temperatures. For the alloys with 0.24% B, the chromium addition lowers the ductility at room temperature. The

Table 8. Effect of surface treatment on room-temperature tensile properties of FA-350 (Fe-35.8Al-0.05Zr-0.24B, at. %)

Surface treatment	Ductility (%)	Yield strength, MPa (ksi)	Tensile strength, MPa (ksi)
1 h/700°C/vac	10.7	325 (47.2)	758 (110)
1 h/700°C/vac + oil coating	13.4	329 (47.8)	847 (123)
30 min/700°C/air, 6 times	14.2	357 (51.8)	923 (134)

Table 9. Effect of chromium additions on tensile properties of FA-342-type alloys

Alloy number	Composition (at. %)	Strength, MPa (ksi)		Elongation (%)
		Yield	Tensile	
<b>Room temperature</b>				
FA-342	0.1Zr + 0.24B	337 (48.9)	740 (107.4)	9.1
FA-370	0.1Zr + 0.24B + 2Cr	329 (47.8)	616 (89.4)	6.2
FA-369	0.1Zr + 0.24B + 5Cr	321 (46.6)	404 (58.7)	2.7
FA-353	0.1Zr + 0.40B + 5Cr	350 (50.8)	608 (88.3)	5.6
<b>600°C</b>				
FA-342		351 (51.0)	368 (53.4)	57.4
FA-370		349 (50.6)	419 (60.8)	41.7
FA-369		334 (48.5)	398 (57.7)	52.6
FA-353		338 (49.1)	413 (59.9)	66.4

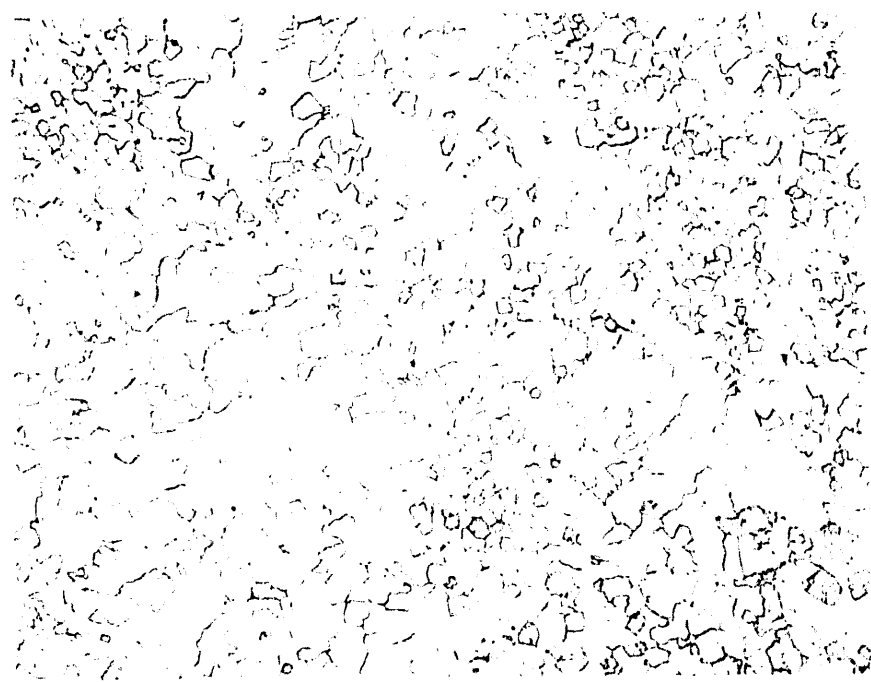


Fig. 8. Fa-369 (Fe-35.8Al-0.1Zr-0.24B-5Cr, at. %) produced by hot extrusion at 900°C and annealed for 1 h at 900°C, 100x.

loss in ductility is partially recovered when the boron level is increased to 0.4% B. All alloys, with and without chromium, are extremely ductile at 600°C.

### 3.4 EFFECT OF VANADIUM IN B-DOPED FeAl (35.8% Al) CONTAINING 5% Cr

Vanadium at a level of 0.5% was added to boron-doped FeAl (35.8% Al) containing 5% Cr for study of its alloying effect. Two alloys, FA-368 and -356, with compositions listed in Table 10 were prepared and fabricated into bar stock. Table 10 shows the tensile properties of the alloys tested at room temperature and 600°C after annealing for 1 h at 900 to 1000°C. The vanadium addition significantly improved the yield strength of FeAl at both temperatures. The ductility appeared to be unaffected by vanadium at room temperature but is lower at 600°C.

Table 10. Effect of 0.5% V on tensile properties of B-doped FeAl (35.8% Al) containing 5% Cr

Alloy number	Composition (at. %)	Strength, MPa (ksi)		Elongation (%)
		Yield	Tensile	
<b>Room temperature</b>				
FA-353	0.4B + 0.1Zr + 5Cr	350 (50.8)	608 (88.3)	5.6
FA-368	0.4B + 0.5V + 5Cr	495 (71.9)	657 (95.4)	4.6
FA-356	0.8B + 0.5V + 5 Cr	511 (74.2)	812 (117.8)	6.6
<b>600°C</b>				
FA-353		338 (49.1)	413 (59.9)	66.4
FA-368		413 (60.0)	506 (73.4)	30.9
FA-356		--	--	--

### 3.5 EFFECT OF MOLYBDENUM ADDITIONS IN FeAl ALLOYS

Molybdenum at levels to 1 at. % was added to FeAl alloys to study its alloying effects. The alloys used to investigate molybdenum effects are listed in Table 11. They were prepared by arc melting and drop casting, followed by hot extrusion at 900°C. All the alloys were fabricated into 9-mm-diam bar stock without difficulty.

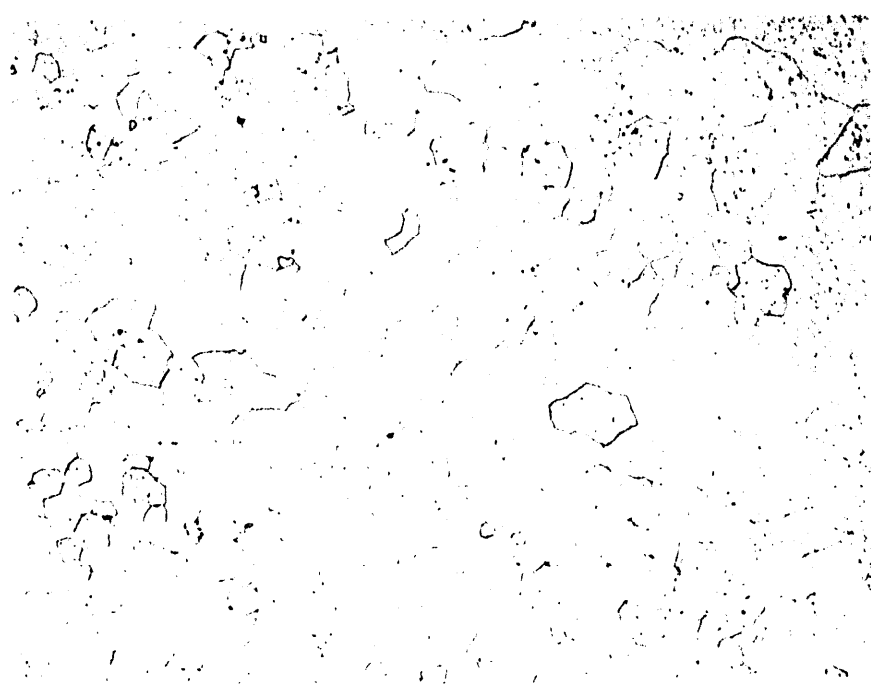
Figure 9 shows a microstructure typical of molybdenum-modified FeAl alloys. Fine particles ( $\sim 1 \mu\text{m}$  in diam) were distributed quite uniformly within grains and along grain boundaries. The chemical compositions of the matrix and particle phases in FA-362, -363, and -364 were determined by electron microprobe analysis with a beam voltage of 20 kV. The results are listed in Table 12. The matrix phase contains no zirconium, indicating that the solubility of zirconium in FeAl is negligible. Molybdenum is depleted slightly in the matrix and is enriched to a level of 2 at. % in particles (I). These particles, possibly  $\text{ZrB}_2$  type, are substantially enriched with zirconium, the level of which is as high as 56% in FA-362. Molybdenum-rich particles (II) [containing  $\sim 22\%$  Mo] are observed only in FA-364 containing 1 at. % Mo, indicating that the solubility of molybdenum in FeAl is less than 1% (probably around 0.9 at. %).

Table 11. Effect of molybdenum additions on tensile properties of FeAl (35.8% Al) alloys

Alloy number	Composition (at. %)	Room temperature			Elongation (%)
		Yield	Strength, MPa (ksi) Tensile		
F-350-1	0.05Zr + 0.24B	325 (47.2)	755 (109.6)	10.7	
FA-362	0.05Zr + 0.24B + 0.2Mo	401 (58.2)	836 (121.3)	11.8	
FA-363	0.05Zr + 0.24B + 0.5Mo	367 (53.2)	754 (109.4)	9.7	
FA-364	0.05Zr + 0.24B + 1.0 Mo	360 (52.3)	679 (98.6)	7.0	
FA-367	0.02Zr + 0.8B + 0.5Mo + 5 Cr	516 (74.9)	841 (122.1)	7.6	
<b>600°C</b>					
FA-350-1		378 (54.9)	360 (52.2)	56.6	
FA-362		424 (61.6)	453 (65.8)	34.3	
FA-363		394 (57.2)	491 (71.2)	35.1	
FA-364		400 (58.0)	492 (71.4)	51.5	
FA-367		446 (64.8)	551 (79.9)	32.9	

Y-803

(a)



Y-842

(b)

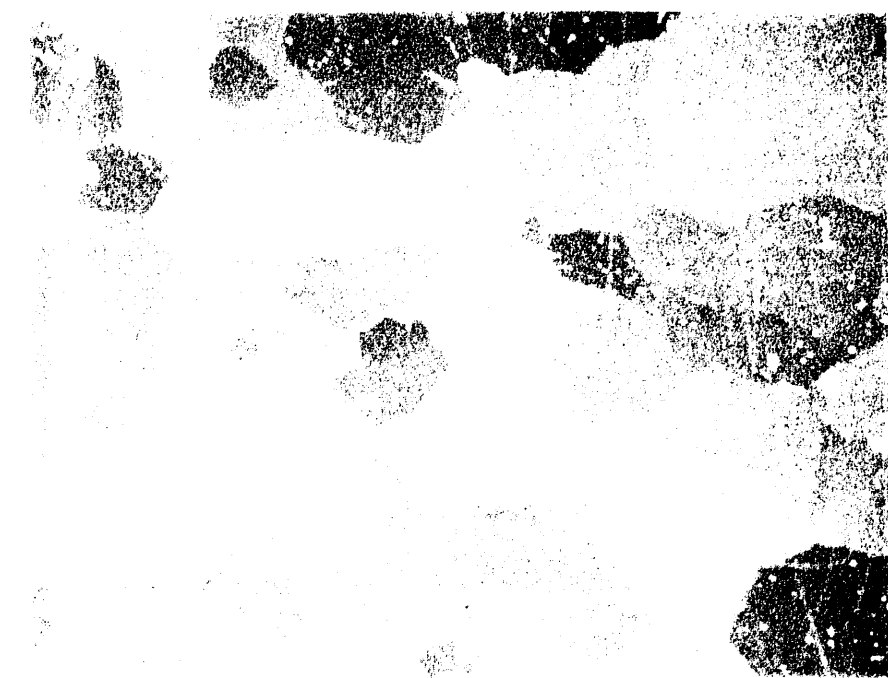


Fig. 9. Microstructure of FA-362 (Fe-35.8Al-0.05Zr-0.24B-0.2Mo, at. %) annealed for 1 h at 800 plus 1 h at 700°C:  
(a) optical micrograph, 200 $\times$ , and (b) back-scattered electron photograph, 780 $\times$ .

Table 12. Electron microprobe analyses of chemical composition of FA-362, -363, and -364 alloys

	FA-362 <sup>a</sup> (at. %)			FA-363 <sup>b</sup> (at. %)			FA-364 <sup>c</sup> (at. %)		
	Al	Mo	Zr	Al	Mo	Zr	Al	Mo	Zr
Matrix	34.61	0.17	0	35.76	0.43	0	35.30	0.85	0
Particle (I)	13.23	1.80	56.17	15.38	2.42	49.59	22.74	1.90	30.64
Particle (II)							23.71	22.36	0.30

<sup>a</sup>Nominal composition: Fe-35.8Al-0.2Mo-0.05Zr-0.24B, at. %

<sup>b</sup>Nominal composition: Fe-35.8Al-0.5Mo-0.05Zr-0.24B, at. %.

<sup>c</sup>Nominal composition: Fe-35.8Al-1.0Mo-0.05Zr-0.24B, at. %

Table 11 summarizes the tensile properties of the molybdenum-modified FeAl alloys tested at room temperature and 600°C. All specimens were annealed at 700 to 900°C prior to tensile testing. Alloying with 0.2% Mo increases both strength and ductility at room temperature. FA-362 has a tensile ductility of 11.8%, the highest tensile ductility ever reported for FeAl alloys with a bare surface. Further increases in molybdenum concentration caused a decrease in room-temperature ductility and strength. Comparison of FA-363 and -367 indicates that alloying with 5% Cr significantly increases the strength at room temperature and 600°C but lowers the ductility at room temperature. All alloys are ductile at 600°C. The tensile results in Table 11 indicate that the optimum level of molybdenum in FeAl is around 0.2%.

#### 4. CREEP PROPERTIES OF FeAl (35.8% Al) ALLOYS

Creep properties of selected FeAl (35.8% Al) alloys were determined by testing at 138 MPa (20 ksi) and 593°C (1100°F) in air. All buttonhead specimens with a dimension of 3.18 mm diam by 17.8 mm long were annealed in vacuum at 700 to 900°C prior to creep testing. The creep strain was measured by a dial gage, and the rupture elongation was determined at room temperature. The applied stress was calculated based on the original cross section of alloy specimens, and no correction was made for the reduction of area during creep testing.

Table 13 summarizes the creep results of FeAl alloys tested at 138 MPa and 593°C. All alloys (except the binary base FA-324) were extremely ductile, with a rupture elongation over 60%. Examination of the creep data in Table 13 reveals the following alloying effects:

1. Addition of boron and zirconium, both of which improve the tensile ductility at ambient temperatures, extends the rupture life of FeAl (35.8% Al) by a factor of about two at 593°C. Vedula and Stephens,<sup>25</sup> on the other hand, reported that alloying with 0.1% Zr and 0.2% B reduced the creep rate of Fe-40% Al by an order of magnitude at 827°C.
2. Alloying with chromium alone or chromium in combination with 0.5% V provides no significant improvement in creep resistance.
3. Molybdenum at a level of 0.2% substantially extends the rupture life and reduces the creep rate of FA-350. Further increases in molybdenum concentration reduce the creep resistance. The alloy FA-362 containing 0.2% Mo showed a rupture life of 894 h, which is longer than that of the binary alloy FA-324 by more than an order of magnitude.
4. A combination of 0.5% Mo and 5% Cr (FA-367) also substantially extends the rupture life of FeAl.

Table 13. Creep properties of FeAl (35.8% Al) alloys tested at 138 MPa (20 ksi) and 593°C (1100°F)

Alloy number	Composition (%)	Rupture life (h)	Minimum creep rate (%/h)	Rupture elongation (%)
FA-324	Base <sup>a</sup>	46.4	0.23	28.0
FA-342-1	0.24B + 0.1Zr	70.9	0.49	101.0
FA-350-1	0.24B + 0.05Zr	106.6	0.22	123.2
FA-370	0.24B + 0.1Zr + 2Cr	73.4	0.45	101.5
FA-369	0.24B + 0.1Zr + 5 Cr	37.6	0.87	>137
FA-353-1	0.40B + 0.1Zr + 5 Cr	104.8	0.27	85.4
FA-368	0.40B + 0.0Zr + 5Cr + 0.5V	130.6	0.17	85.6
FA-356-1	0.80B + 0.0Zr + 5Cr + 0.5V	164.1	0.20	80.9
FA-362	0.24B + 0.05Zr + 0.2Mo	894.3	0.031	87.7
FA-363	0.24B + 0.05Zr + 0.5Mo	209.7	0.16	98.6
FA-364	0.24B + 0.05Zr + 1.0Mo	159.0	0.126	75.6
FA-367	0.80B + 0.0Zr + 0.5Mo + 5Cr	710.0	0.040	63.8

<sup>a</sup>Fe-35.8 at. % Al.

Based on these limited results, we assert that the creep resistance of FeAl can be effectively improved by alloying with 0.2% Mo or a combination of 0.5 Mo and 5% Cr. Molybdenum was also found to be effective in improving the creep properties of  $\text{Fe}_3\text{Al}$ , and its beneficial effect was highly dependent on other alloying additions.<sup>10,22</sup>

## 5. OXIDATION PROPERTIES

Oxidation properties of FeAl (35.8%) alloys were determined by exposure to air for up to 500 h at 800 and 1000°C. Disk specimens were first recrystallized for 1 h at 900°C in vacuum prior to air exposure. The specimens were periodically removed from the furnace and cooled to room temperature for weight measurements.

Figures 10 and 11 show the plot of weight change in FA-350 (Fe-35.8Al-0.05Zr-0.24B, at. %), FA-362 (Fe-35.8Al-0.05Zr-0.24B-0.2Mo), and FA-375 (Fe-3.5.8Al-0.05Zr-0.24B-0.2Mo-2.0Cr) as a function of exposure time at 800 and 1000°C, respectively. At 800°C, the base alloy FA-350 showed a variation of weight increase and decrease during exposure, while FA-362 and -375 containing 0.2% Mo exhibited a steady weight gain for 500-h exposure. The weight gain is due to formation of oxide scales, and weight loss is apparently associated with oxide spalling. In terms of net weight change, all three alloys showed a comparable weight gain after a 500-h exposure at 800°C.

The base alloy FA-350 showed a substantial weight loss while FA-362 and -375 exhibited a weight gain after 500 h-exposure at 1000°C (see Fig. 11). This result clearly indicates that alloying with 0.2% Mo enhances scale adherence and therefore improves oxidation resistance of FeAl. It is interesting to point out that FA-362 and -375 showed less weight gain at 1000 than at 800°C. This probably results from a rapid formation of  $\alpha$ -alumina scales, which more effectively protect the base metal from excessive oxidation. Similar oxidation behavior has been observed in nickel aluminide alloys based on  $\text{Ni}_3\text{Al}$  (ref. 26).

## 6. PREPARATION, FABRICATION, AND EVALUATION OF LARGE FeAl ALLOY HEATS

### 6.1 MELTING OF FeAl ALLOYS

The initial FeAl composition (FA-350) meeting the room-temperature ductility requirement was scaled up at Oak Ridge National Laboratory (ORNL) to 7.5-kg (15-lb) heats. The alloy was processed by vacuum-induction melting (VIM) in a  $\text{ZrO}_2$  crucible.

ORNL-DWG 92-11979

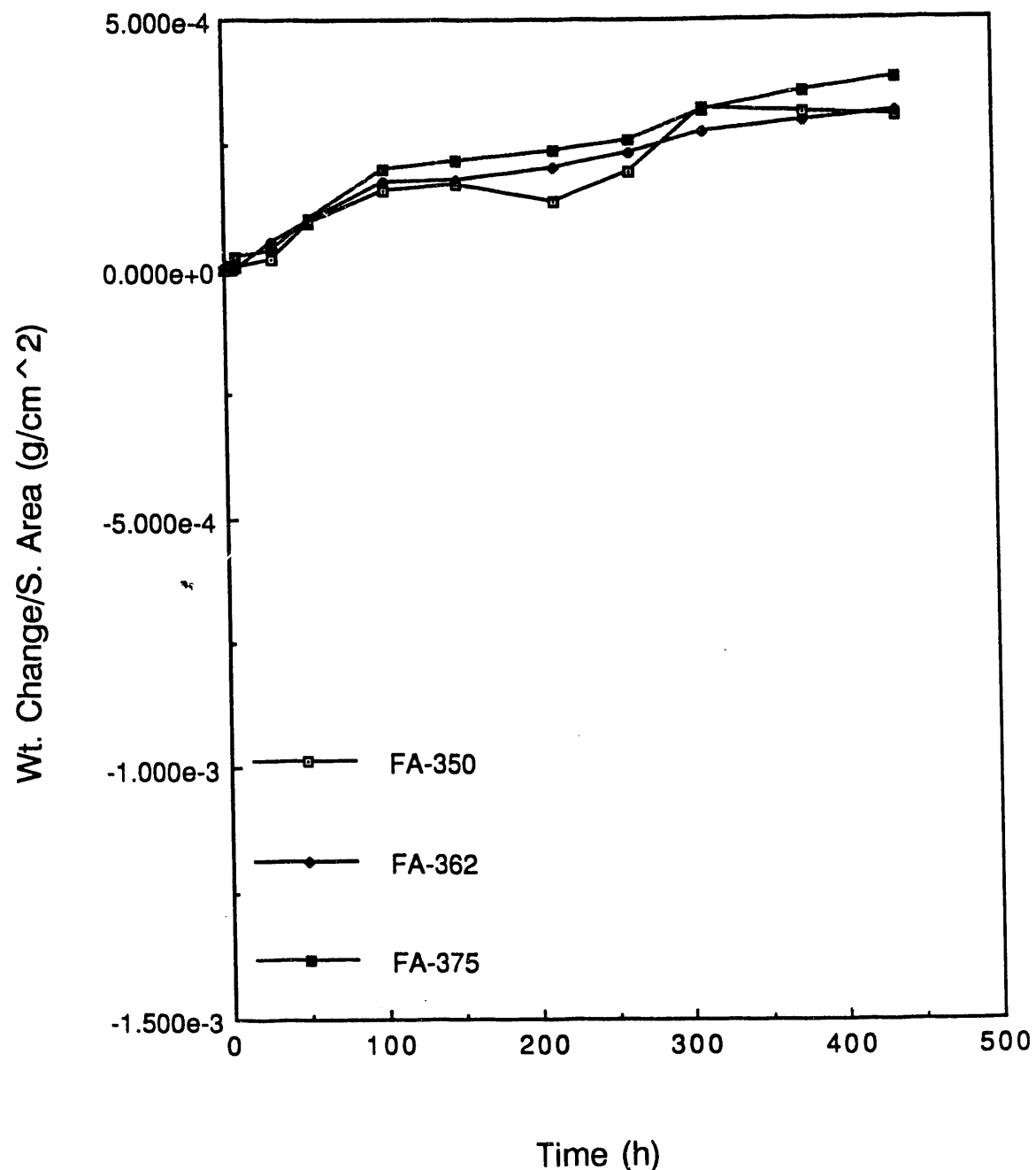


Fig. 10. Plot of weight change as a function of exposure time for FeAl alloys exposed to air at 800°C.

ORNL-DWG 92-11980

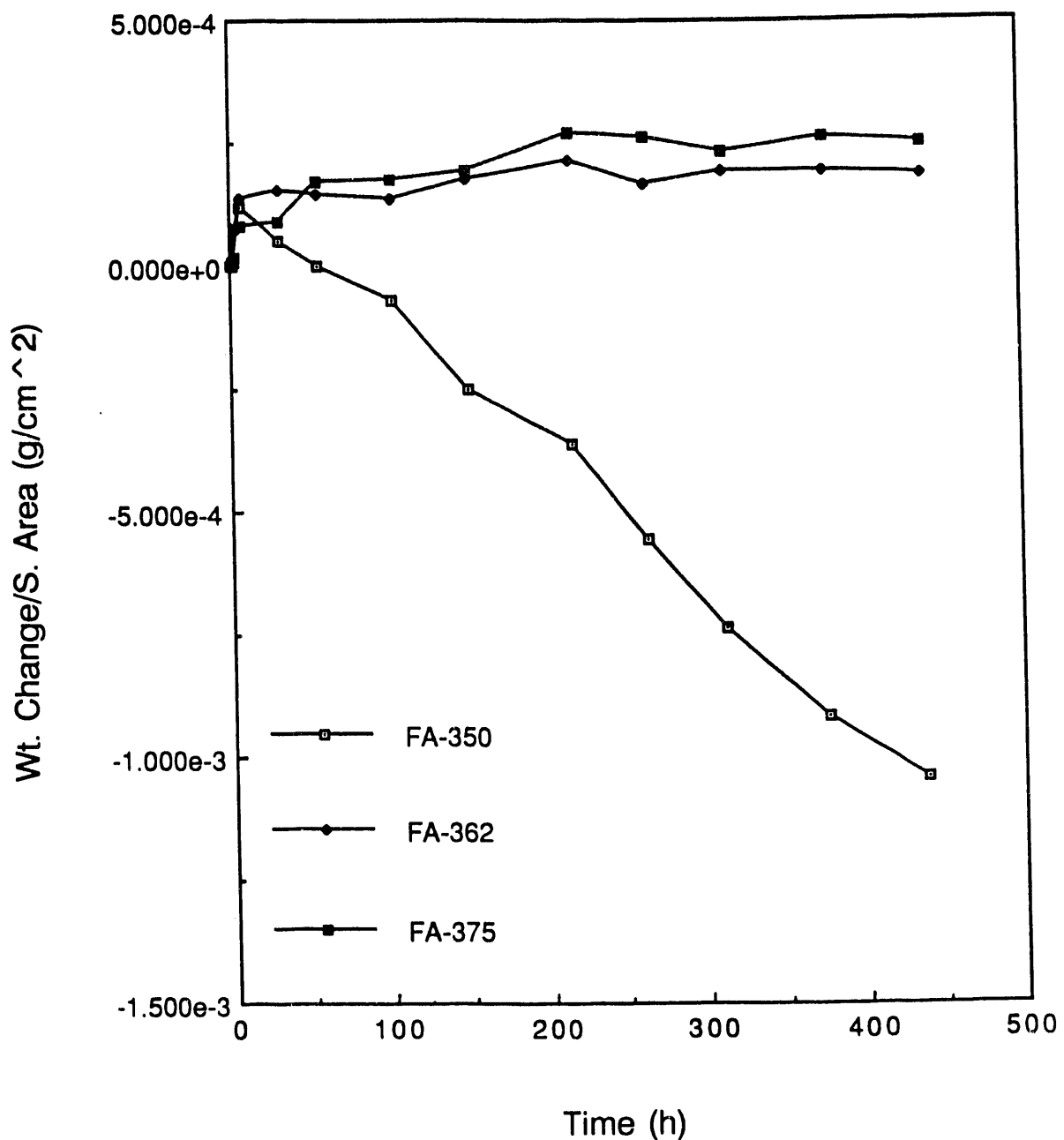


Fig. 11. Plot of weight change as a function of exposure time for FeAl alloys exposed to air at 1000°C.

The melt stock was electrolytic iron and high-purity aluminum chips. The electrolytic iron was hydrogen fired at 1000°C to reduce any surface oxide and was stored in a desiccator prior to use. The aluminum chips were cleaned in 10% HNO<sub>3</sub> solution, washed in water followed by alcohol, blow dried, and also stored in a desiccator. The aluminum and iron were alternately stacked in the crucible with zirconium and boron additions hidden near the bottom. With the increase in power of the induction unit, aluminum melts and starts to dissolve iron, zirconium, and boron. Some increase in temperature occurs from the exothermic nature of the dissolution of iron in aluminum. The temperature is finally brought up to 1500°C and molten metal poured into a 72-mm-diam graphite mold. The ingot is allowed to cool in vacuum prior to removal. No significant reaction of FeAl alloy with the ZrO<sub>2</sub> crucible was observed. However, the FeAl alloys showed slightly more reaction with the ZrO<sub>2</sub> crucible than Ni<sub>3</sub>Al-based alloys. The ingot surface was smooth in all cases. The hot tops of the ingots were cut using a band saw. Similar cutting using an abrasive cut-off wheel tended to produce cracks on the cut surface. The cracking tendency could be minimized by using a coolant containing water-soluble oil. The pieces cut with the band saw were always free of any surface cracks. Several ingots of FeAl are shown in Fig. 12. The FA-350 composition of FeAl was also arc melted and cast into 25-mm-diam by 125-mm-long ingots in copper molds. These ingots were cut into sections for hot compression testing.

The modified FA-350 composition (FA-362) with improved mechanical properties was also scaled up at ORNL to 7.5-kg (15-lb) heats. The same procedure as previously described for VIM of FA-350 was used except that the melting and casting was carried out in air. Once again, the ingots were of excellent surface finish. No indications of shrinkage or gas porosity were observed.

The FA-350 and an earlier composition (FA-328: Fe-35.8% Al-5% Cr-0.1% Zr-0.12% B) were scaled up to 40-kg (80-lb) heats at Haynes International. The alloys were VIM processed into 76-mm-diam electrodes. These electrodes were subsequently electroslag remelted (ESR) into 102-mm (4-in.)-diam ingots. These ingots are shown in Fig. 13. The Haynes-reported composition of FA-350 ingots is compared with the target composition in Table 14. Note that the ESR ingots of both FA-328 and -350 had excellent surface finish.

In addition to the melting of FeAl alloys at ORNL and Haynes International, melting attempts were also made at Timken. The first attempt was to melt a 250-kg (500-lb) heat by the air-induction-melting (AIM) process, and casting into a 205-mm (8-in.)-square ingot. This AIM ingot was found to contain an enormous amount of large porosity

YP11197

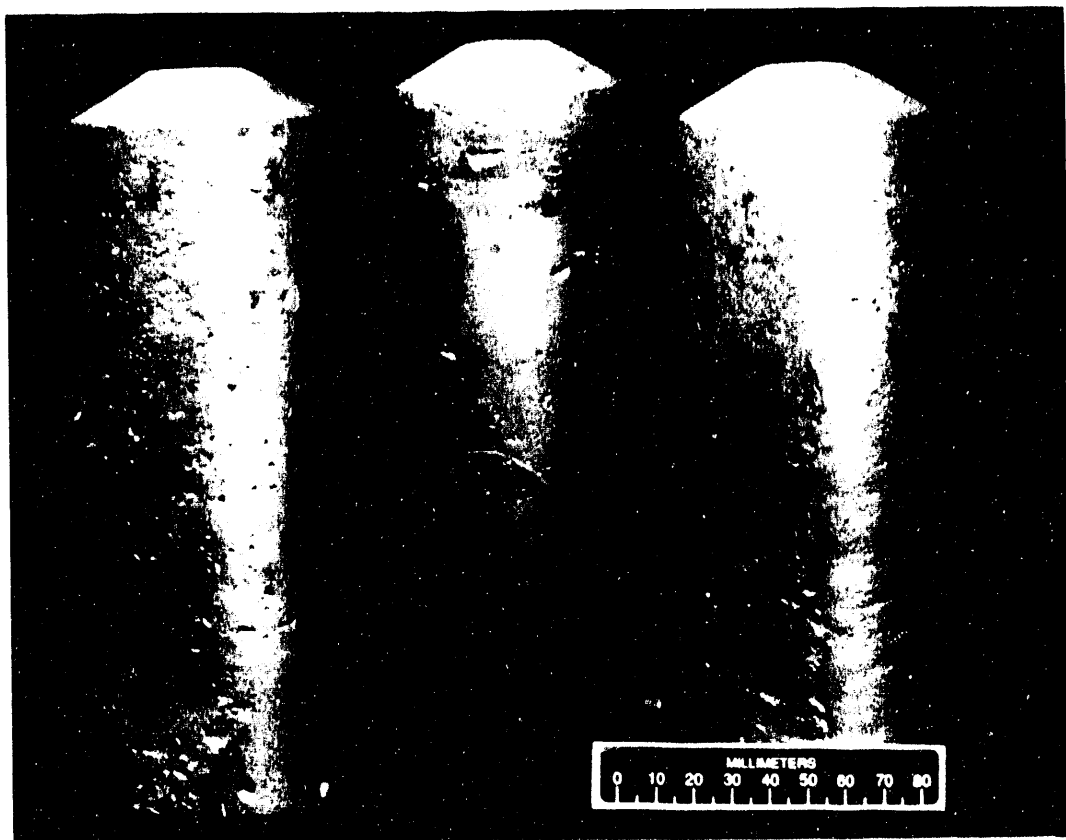


Fig. 12. Photograph showing 7.5-kg (15-lb) ingots of FeAl alloys (FA-328, -350, and -362) melted and cast at ORNL. Ingots were melted by air- and vacuum-induction melting in a  $ZrO_2$  crucible. Note the good surface quality.

YP9510

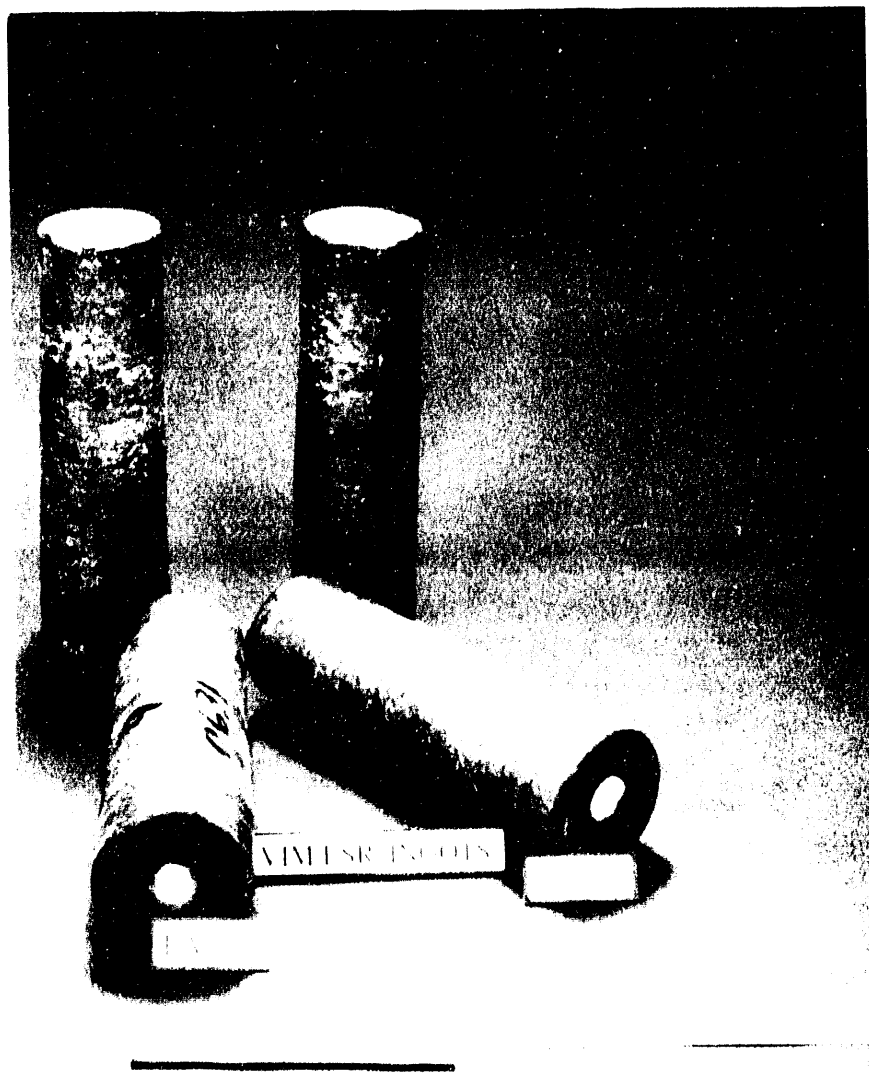


Fig. 13. Photograph showing ingots from 40-kg (80-lb) heats of FeAl alloys (FA-328 and -350) melted at Haynes International. The alloys were vacuum-induction melted, followed by electroslag remelting. Note the excellent surface quality.

Table 14. Chemical analysis of alloy FA-350 prepared by electroslag remelting at Haynes International

Element	Weight percent	
	Target	Vendor analysis <sup>a</sup> (heat 11-0-640)
Al	21.21	21.19
Cr	--	--
Zr	0.10	0.13
B	0.06	0.06
Fe	78.63	78.62

<sup>a</sup>Other elements which are typically analyzed during check analysis were not reported by the vendor.

(see Fig. 14). In fact, Timken observed the swelling of the ingot hot-top rather than the normal behavior of hot-top shrinkage. The ingot porosity and hot-top swelling indicated that large amounts of gases were trapped in molten metal. The escaping gas caused sufficient pressure to cause the hot-top swelling. The exact nature of the gas is not known. It might be dissolved oxygen or hydrogen. After this observation, Timken melted two 50-kg (100-lb) heats by VIM and cast the molten metal into 102-mm (4-in.)-diam tapered ingots. The hot-top swelling observed during AIM disappeared, and the ingots were essentially porosity free (see Fig. 15). It is believed that the VIM process pumped the porosity-causing gas out of the liquid prior to pouring into the mold. Target and check analyses of the Timken heats are presented in Table 15. All the target elemental concentrations were met in the heats melted by Timken. The cutting processes used at Timken produced cracked faces of all four ingots that were sent to ORNL for subsequent processing. The cracked ends of the Timken ingots were removed by a band saw by cutting approximately 12-mm (1/2-in.)-thick slices from each end of each of the ingots.

## 6.2 PROCESSING OF FeAl ALLOYS

The initial processing of FeAl alloys was conducted on 25-mm (1-in.)-diam ingots produced by AIM at ORNL. The round ingots were cut into 37-mm (1-1/2-in.)-long specimens for compression testing. The nickel-aluminide dies and the FeAl specimens were both heated at temperatures of 800, 900, 1000, and 1100°C. The heated dies and specimens were compressed nearly 85% in one step. All forging temperatures produced compressed specimens free of any defects. The starting specimen and the compressed pieces are shown in Fig. 16. This figure implies that FeAl alloys should be forgeable at a temperature range of 800 to 1100°C, provided the dies are heated.

YP11180



Fig. 14. Photograph showing a section of an ingot cast from 250-kg (500-lb) heat of FeAl alloy (FA-328) melted at The Timken Company. The alloy was air-induction melted and cast into a 200-mm (8-in.)-square ingot. Note the large porosity in the ingot.

YP11179

## VACUUM-MELTED INGOT



Fig. 15. Photograph showing a section of an ingot cast from a 50-kg (100-lb) heat of FeAl alloy (FA-328) melted at The Timken Company. The alloy was prepared by VIM and cast into a 100-mm-diam tapered ingot. Note the absence of any porosity compared to that observed in air melting.

Table 15. Target and check analysis of alloy FA-350  
vacuum-induction melted at The Timken Company

Element	Weight percent		
	Target	Ingot 176B	Ingot 177B
Al	21.21	20.9	21.0
Cr	--	0.07	0.03
Zr	0.10	0.09	0.09
B	0.06	0.05	0.051
C	--	0.044	0.034
Mn	--	0.14	0.13
P	--	0.001	0.001
S	--	0.003	0.002
Si	--	0.22	0.21
Ni	--	0.01	0.01
Mo	--	0.01	<0.01
Nb	--	0.01	<0.01
Cu	--	0.11	0.10
N <sub>2</sub>	--	0.002	0.001
O <sub>2</sub>	--	0.001	0.001
Fe	78.63	78.20	78.2

<sup>a</sup>Analysis conducted at ABB-CE (formerly Combustion Engineering),  
Chattanooga, Tenn.

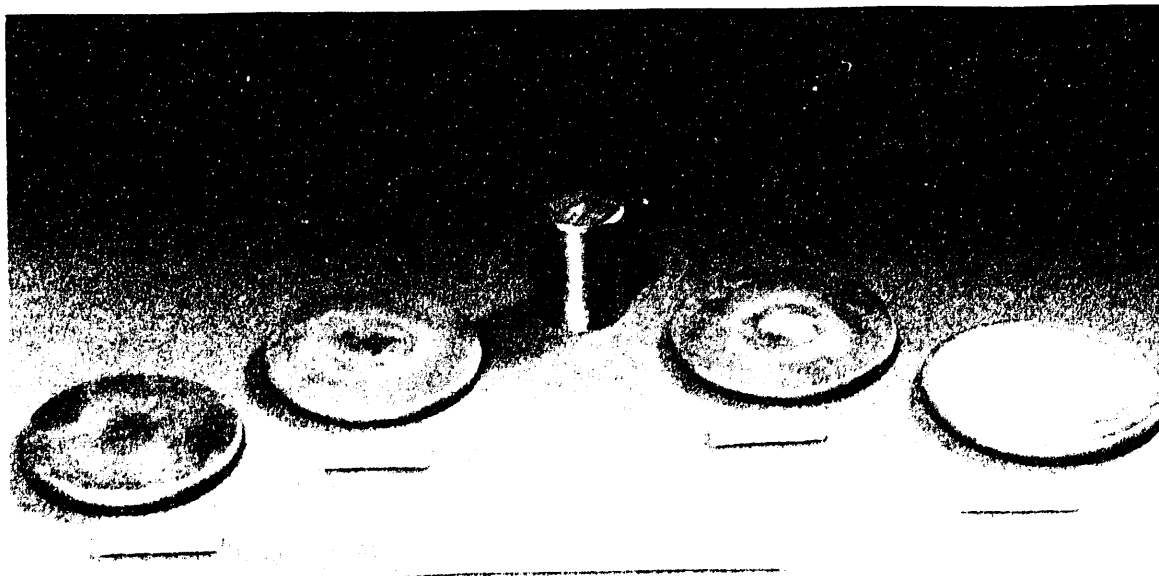


Fig. 16. Photograph showing specimen prior to and after hot compressing over 85% in height at temperatures of 800, 900, 1000, and 1100°C. The specimens and the dies were both heated to the same temperature. The compression tests were performed at ORNL.

### 6.2.1 Hot Forging

Attempts were made to hot forge at ORNL the cast ingots without the use of heated dies at 1000 and 1100°C. In each case, the heat loss to the cold dies caused the contact surfaces to contain cracks. However, when the dies were heated, the ingots could be forged successfully. This observation implies that for the cast ingots, the dies need to be preheated. From the compression results in Fig. 16, the preheating temperature for the dies is estimated to be 800°C.

### 6.2.2 Hot Extrusion

The cast ingots of EA-350 alloys were also subjected to processing by the extrusion process. The initial extrusions were of the bare ingot at 1000°C. The dies were of round and rectangular cross section. In each case, most of the extrusion surface was acceptable. However, each extrusion showed a narrow longitudinal band of shallow cracks. It is believed that the cracks are produced on the surface that comes in contact with the extrusion liner and, thus, some heat is lost. This was confirmed by wrapping the ingots with a 0.76-mm-thick foil sheet of carbon steel. The wrapped ingots produced crack-free

extrusions every time, implying that the 0.76-mm-thick foil sheet of steel was acting as a barrier to heat loss between the ingot and the liner. Successful extrusions with reduction ratios of 4 to 1, 9 to 1, and 12 to 1 were demonstrated at 900, 930, and 1000°C. The extrusion process produces nearly uniform grain-size equiaxed microstructure for a reduction ratio of  $\geq 12$  to 1 (see Fig. 17). However, the extruded microstructure is not uniform for a reduction ratio of  $\leq 4$  to 1 (see Fig. 18). The remnants of the 0.76-mm-thick wrap on the extrusion could be removed easily by dissolving the wrap in a 10% solution of nitric acid.

Several samples from the extruded bars were forged successfully at 1000°C without heated dies. This suggests that once the cast structure is refined, the temperature below which the surface cannot be allowed to cool is significantly reduced. In other words, the forging window is broadened for a fine-grained material.

The nominal 102-mm (4-in.)-diam tapered ingots from Timken were also extruded at ORNL to produce 19-mm-diam bar for hot-twist testing at Timken. The Timken ingots were too large for our 102-mm (4-in.) liner and too small for our 140-mm (5-1/2-in.) liner in the extrusion press. Instead of machining the ingots, it was decided to encase them in a 140-mm-OD and 114-mm-ID pipe of carbon steel. Carbon-steel extrusion noses were welded to the front of each pipe. The 140-mm-diam billets of FA-350 were hot extruded at 1000°C through a 76-mm (3-in.)-diam die. Because of a fairly thick can, the extrusions were of good quality. Each extrusion was cut into three billets of about 205-mm (8-in.) length. The 76-mm-diam billets were further hot extruded at 1000°C through a 25-mm-diam die. The microstructure of the Timken-extruded bar is shown in Fig. 19. The microstructure of an extruded bar with the same diameter but from a 76-mm-diam ingot cast at ORNL is shown in Fig. 20 for comparison. The high-magnification micrographs from the two bars are shown in Fig. 21. These micrographs show that the Timken-melted material contained a large number of second-phase particles both in the matrix and at the grain boundaries. In comparison, the grain boundaries in the ORNL material were free of second-phase particles. Furthermore, the matrix precipitates were finer in size and lower in density in the ORNL material.

One attempt to produce hot-extruded tubing from an AIM ingot of FA-362 was made. The alloy was cast into a solid ingot of 72-mm (2.85-in.) diam. A 25-mm-diam hole was electrodischarge machined into the ingot. The outside of the ingot was wrapped in a 0.76-mm-thick sheet of carbon steel. The ingot was hot extruded at 1100°C over a mandrel into tubing. The hot-extruded tubing and a piece after acid cleaning are shown in Fig. 22. The tubing's outer surface was generally good. However, the inner surface was fairly

YP16405

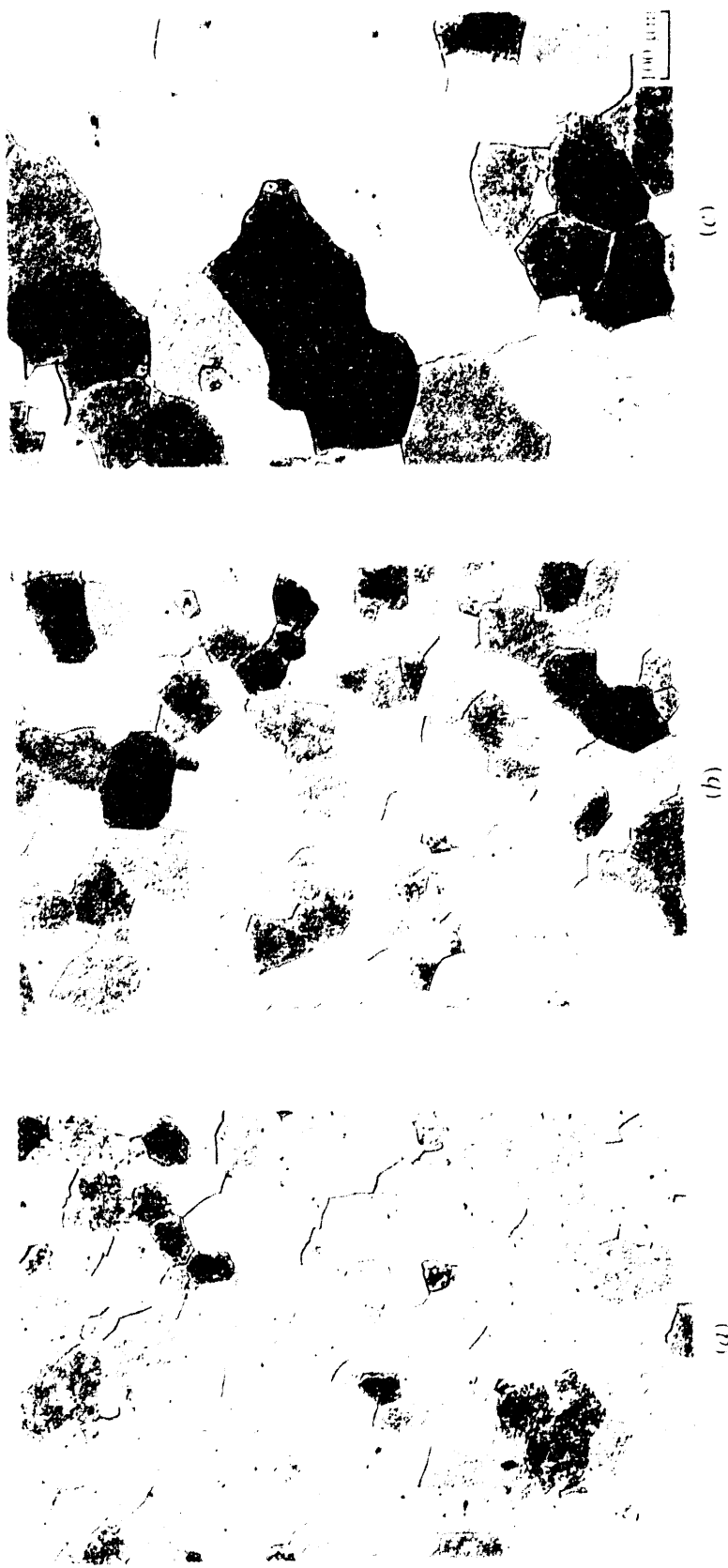


Fig. 17. Optical microstructure of hot-extruded bar of FA-350. The ingot was prepared by VIM at ORNL and extruded in a steel wrap at 930°C to an area reduction ratio of 12 to 1: (a) shows the bar edge, (b) one-half radius, and (c) bar center locations for a transverse section.

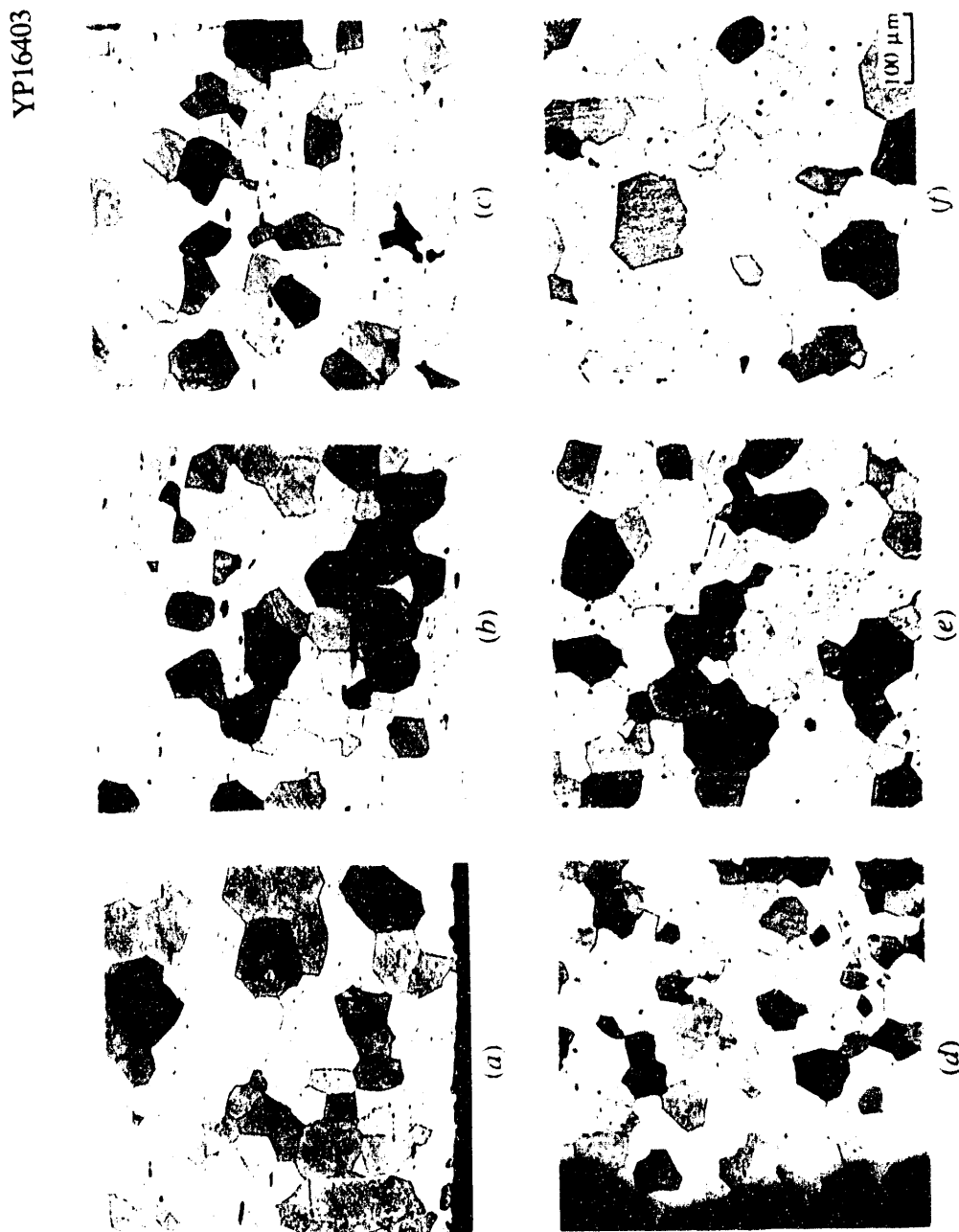


Fig. 18. Optical microstructure of hot-extruded rectangular bar of FA-362. The ingot was prepared by VIM at ORNL and extruded in a steel wrap at 1000°C to a reduction ratio of 4 to 1: (a) shows the bar edge, (b) mid thickness, and (c) other edge of longitudinal section, and (d), (e), and (f) show the same locations for the transverse section.

YP16402

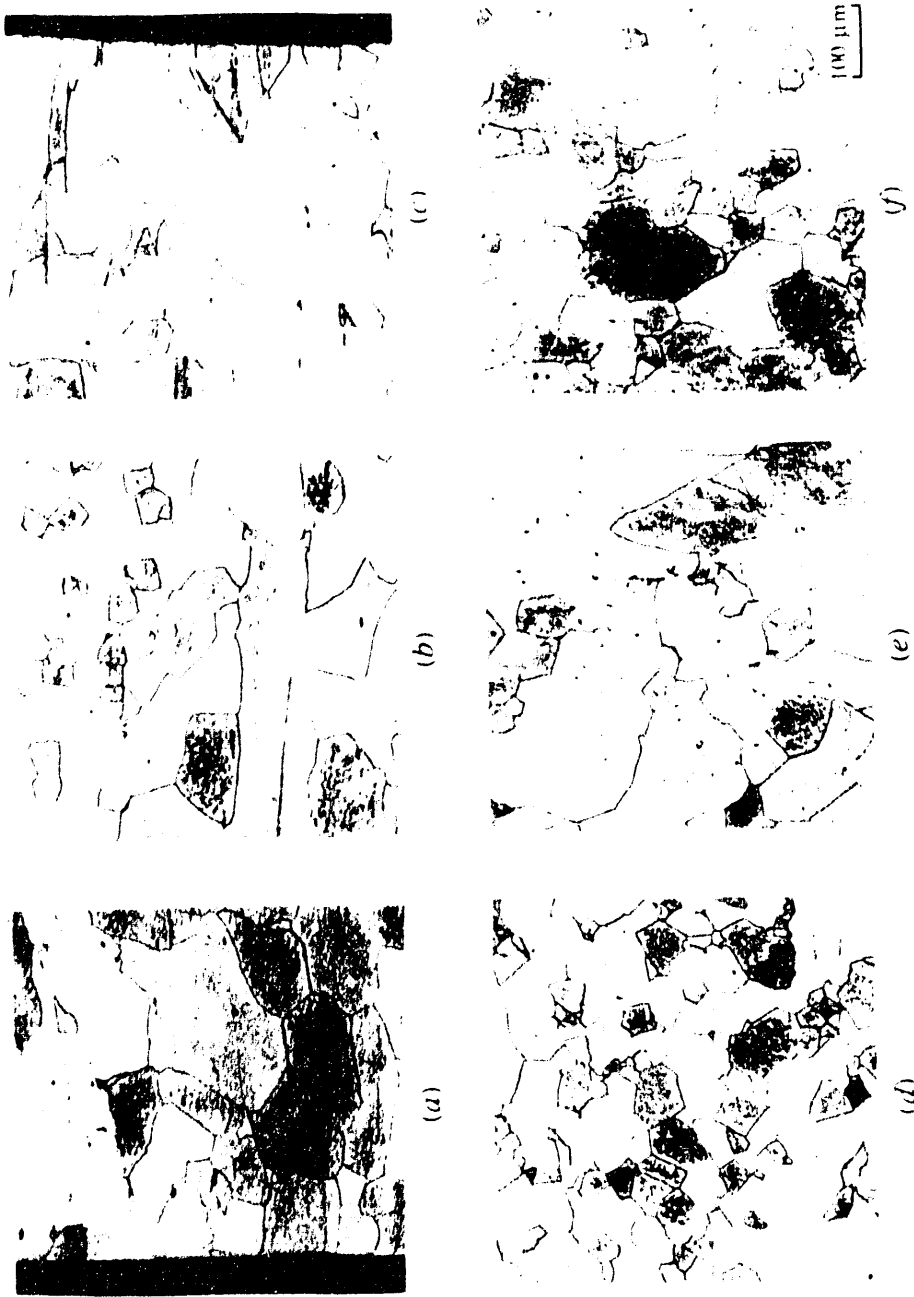


Fig. 19. Optical microstructure of hot-extruded bar of FA-350. The ingot was prepared by VIM at The Timken Company and extruded in a steel can in two steps to a 25-mm-diam bar. The area reduction ratios for steps 1 and 2 were 3.35 and 9 to 1, respectively: (a) shows the bar edge, (b) one-half radius, and (c) bar center locations.

YP16407

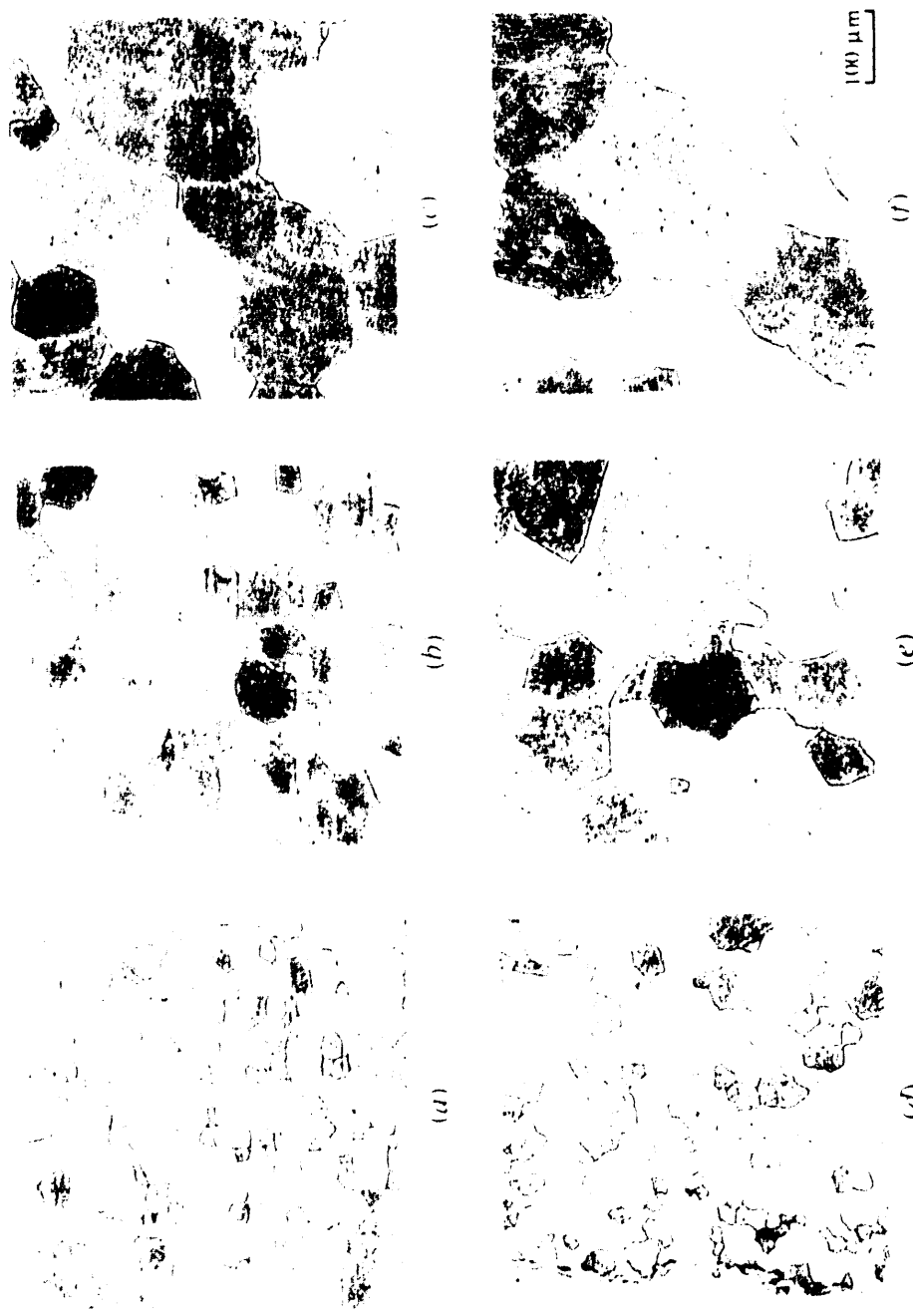


Fig. 20. Optical microstructure of hot-extruded bar of FA-350. The ingot was prepared by VIM at ORNL and extruded in a steel wrap at 1000°C to an area reduction ratio of 9 to 1: (a) shows the bar edge, (b) one-half radius, and (c) bar center locations for the longitudinal section, and (d), (e), and (f) show the same locations for the transverse section.

YP16404



Fig. 21. Comparison of high-magnification micrographs of 25-mm-diam bars of FeAl alloy FA-350: (a) and (b) are transverse sections of Timken- and ORNL-melted materials.

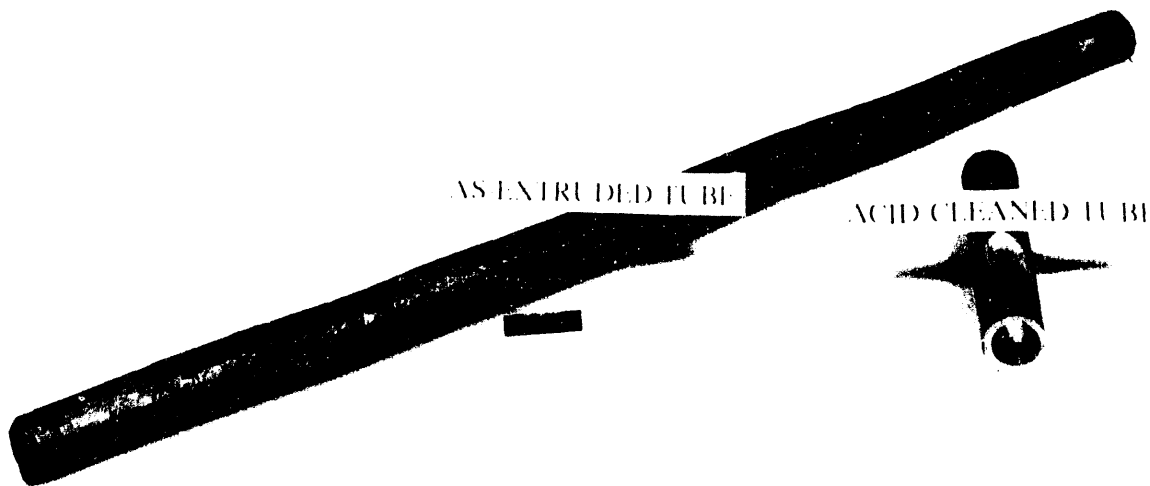


Fig. 22. Photograph showing the tubing of FA-362 in the as-extruded condition and a piece of it after acid cleaning. The tube was extruded in a steel wrap at 1100°C from air-induction-melted ingot at ORNL.

rough. Once again, the cause for rough inner surface is believed to be the heat loss to the cold mandrel. The inner surface of the tube has a significant potential for improvement by either using a heated mandrel or lining the inside surface with a 0.76-mm-thick foil of carbon steel. Both of these possibilities are currently being tried. The microstructure of the as-extruded tube is shown in Fig. 23. Note that besides the quality of the tube surface, the grain structure was fine and uniform across the thickness of the tube. This is true for both the longitudinal and transverse sections.

#### 6.2.3 Hot Rolling

Attempts to bare hot roll either the extruded or hot-forged samples were not successful. The rolling temperatures were 800, 900, and 1000°C. However, the cracking problem during hot rolling was eliminated by covering the work pieces in a 0.76-mm-thick sheet of mild steel. Once covered, hot rolling at 800°C was carried out to produce 0.76-mm-thick sheet from both alloys (FA-350 and -362). An optical microstructure of the hot-rolled, 0.76-mm-thick sheet of FA-362 is shown in Fig. 24. Note that the sheet has an equiaxed fine-grained microstructure in both longitudinal and transverse orientations.

YP16406

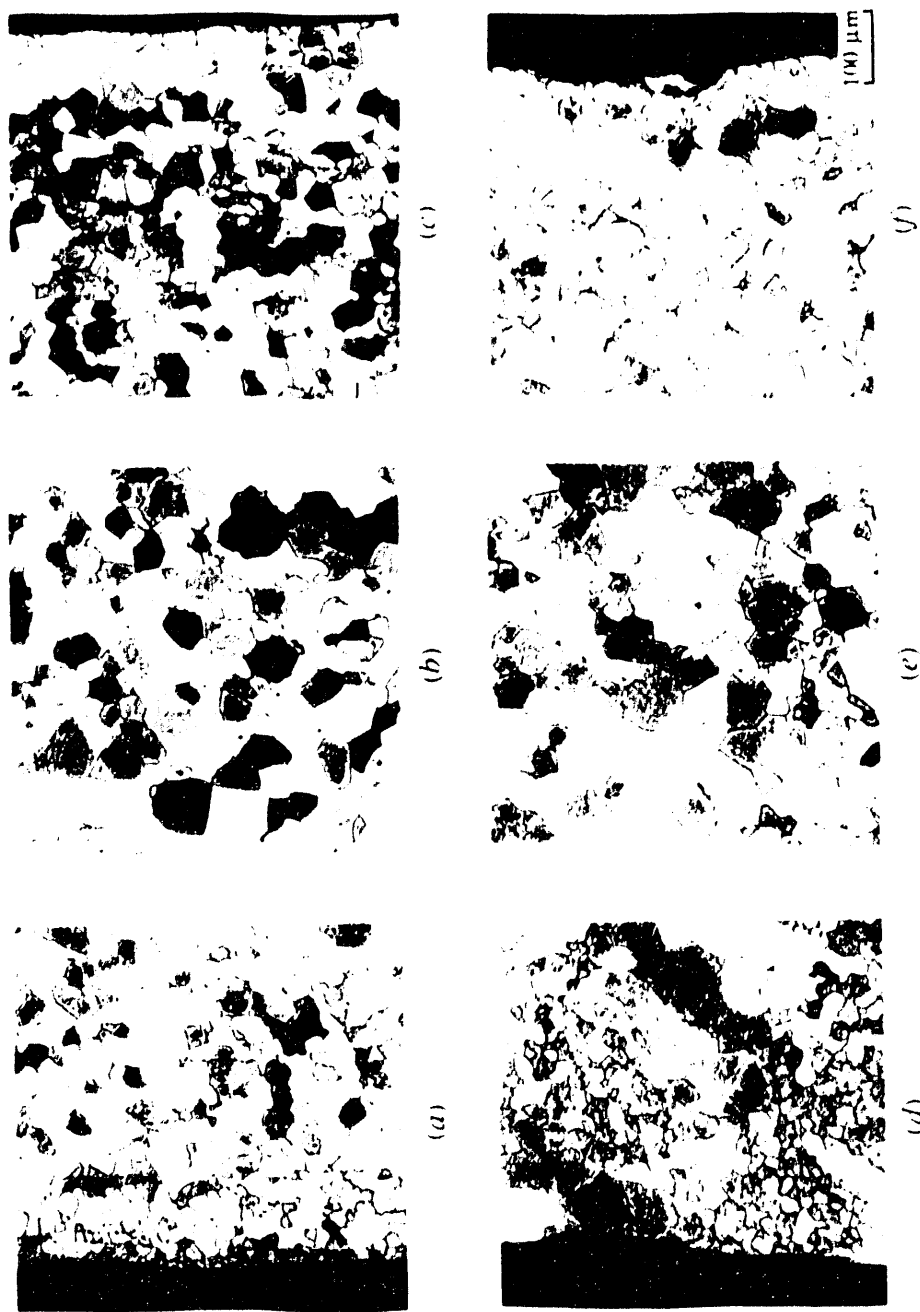


Fig. 23. Optical microstructure of the tubing of FA-362 in the as-extruded condition: (a) shows OD, (b) mid thickness, and (c) ID locations of longitudinal cross section of the tube, and (d), (e), and (f) are OD, mid thickness, and ID locations, respectively, of transverse cross section of the tube.

YP16408

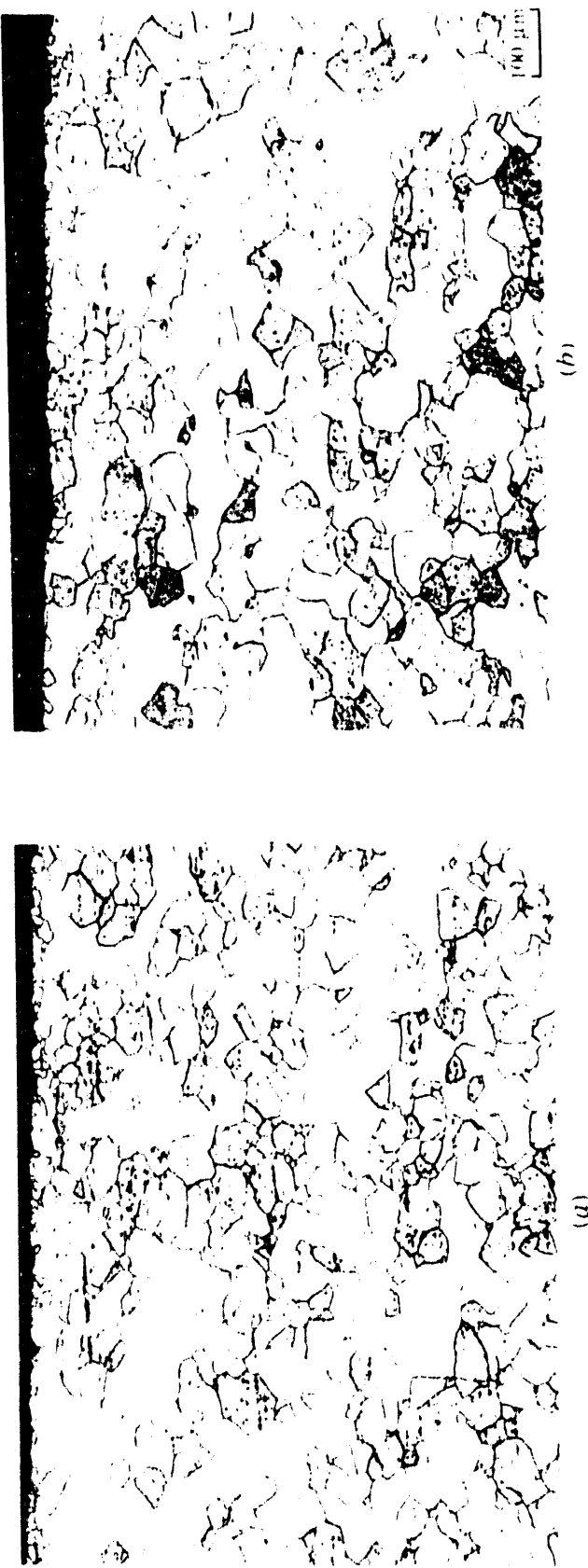


Fig. 24. Optical microstructure of the 0.76-mm-thick sheet of FA-362 in the as-rolled condition: (a) and (b) are the longitudinal and transverse directions of the sheet.

### 6.3 TENSILE TESTING

Tensile specimens of 6.2-mm (0.25-in.) diam and 25-mm (1-in.) length were machined from extruded bar stock. The machined specimens were heat treated at 700°C for 1 h, followed by oil quenching. The specimens were tensile tested at room temperature and a strain rate of  $3.33 \times 10^{-3}/\text{s}$ . Data from these tests are shown in Table 16. Results in this table show that the ingot extruded at 1000°C had better room-temperature ductility than that extruded at 900 or 930°C. Based on these results, the extrusion temperature for all of the ingots was set at 1000°C. Table 16 indicates that the sheet material produced by 1000°C hot extrusion and forging, followed by hot rolling at 800°C, shows the best tensile ductility (= 11%) at room temperature.

Table 16. Tensile properties of hot-extruded bar of FA-350 iron-aluminide alloy. The alloy was prepared by VIM and cast into 72-mm (2.85-in.)-diam ingots. The ingots were hot extruded in a steel wrap at 930 and 1000°C to an area reduction ratio of 12 to 1. Specimens were given an annealing treatment at 700°C for 1 h followed by oil quenching. Data on the bar extruded at 1000°C, forged at 1000°C, and hot rolled into sheet at 800°C are also included for comparison. All of the tests were done in air at a strain rate of  $3.33 \times 10^{-3}/\text{s}$ .

Specimen	Test temperature (°C)	Strength, MPa (ksi)		Ductility, %	
		Yield	Ultimate tensile	Total elongation	Reduction of area
<b>Extrusion temperature 930°C (heat 13700)</b>					
1L	25 <sup>a</sup>	423 (61.4)	721 (104.5)	5.82	6.62
2L	25 <sup>b,c</sup>	417 (60.5)	609 (88.3)	3.70	4.58
<b>Extrusion temperature 1000°C (heat 13688)</b>					
3L	25 <sup>a</sup>	413 (59.9)	762 (110.6)	7.28	6.73
5L	25 <sup>b</sup>	418 (60.6)	737 (106.9)	7.66	7.80
<b>Extruded at 1000°C, forged at 1000°C, rolled at 800°C (heat 13740)<sup>d</sup></b>					
1L	25 <sup>a</sup>	375 (54.4)	703 (102.0)	11.56	10.29
2L	25 <sup>a</sup>	362 (52.6)	687 (99.7)	10.54	12.04

<sup>a</sup>Strain rate = 0.2/min.

<sup>b</sup>Strain rate = 0.05/min.

<sup>c</sup>Specimen broke at extensometer gage mark.

<sup>d</sup>Sheet specimens 0.76 mm thick.

The 0.76-mm-thick, hot-rolled sheets of FA-350 and -362 from 7.5-kg (15-lb) heats were also tensile tested in the temperature range of room temperature to 800°C. The hot-rolled sheets were stress relieved at 700°C for 1 h, followed by oil quenching. The stress-relieved sheets were die punched into 13-mm gage-length tensile specimens. Punched specimens were given a 1-h anneal at 700°C, followed by oil quenching. Tensile data on these specimens are summarized in Tables 17 and 18. The strength and ductility data on alloys FA-350 and -362 are plotted in Figs. 25 through 28. Note that the yield strength of these alloys stays fairly high (at least 320 MPa) to 600°C. The ultimate tensile strength values were closely related to total elongation. If full elongation values were reached, the ultimate tensile strength values were high. The overall elongation values of the 7.5-kg (15-lb) heats were generally lower than 10% for test temperatures up to 500°C. At 500°C and higher, elongation and reduction of area values increase sharply. The sharp drop in ductility below 600°C indicates the necessity of cover during hot rolling. Strength and ductility properties of alloys FA-350 and -362 are compared in Figs. 29 through 32. Note that the two alloys have very similar behavior in strength properties. However, the ductility values of FA-362 are somewhat lower than FA-350 at temperatures of 600°C and above. The lower ductilities of FA-362 are possibly caused by air melting of the alloy ingot versus vacuum melting for FA-350.

## 7. SUMMARY AND CONCLUSIONS

The initial development of FeAl for structural use in corrosive environments at elevated temperatures contained four parts: (1) selection of a base binary composition of FeAl for alloying studies, (2) improvement in metallurgical and mechanical properties of FeAl by control of microstructure and alloy additions, (3) preparation and evaluation of large heats with optimum compositions, and (4) evaluation of corrosion properties of FeAl alloys exposed to molten salt environments at elevated temperatures. This report summarizes the results from the first three parts, and those from the fourth part were reported previously by Tortorelli and Bishop.<sup>12</sup> The first results from a study of the weldability of FeAl alloys are not included in this report.

Mechanical properties of FeAl are sensitive to the aluminum level in the aluminide. The first phase of this development is to determine an optimum level of aluminum in FeAl for alloying studies. Alloy ingots containing 30 to 43 at. % Al were prepared by arc melting and drop casting, and all of them were successfully fabricated into sheets by hot

Table 17. Tensile properties of 0.75-mm steel specimens of 7.5-kg (15-lb) heat of FA-350 alloy. The heat was vacuum-induction melted and cast into a 72-mm-diam ingot. The ingot was extruded at 1000°C in a mild steel wrap into a 25-mm-diam bar. The bar was forged flat at 1000°C and hot rolled in a steel cover at 800°C to a thickness of 0.76 mm. The sheet was stress relieved at 700°C for 1 h, followed by oil quenching. The punched specimens were annealed for 1 h at 700°C, followed by oil quenching.

Specimen	Test temperature (°C)	Strength, MPa (ksi)		Ductility, %	
		Yield	Ultimate tensile	Total elongation	Reduction of area
9L	RT	356 (51.65)	635 (92.03)	7.08	8.94
10L	RT	398 (57.72)	688 (99.84)	9.10	10.06
11L	100	337 (48.81)	530 (76.84)	5.48	8.38
12L	200	333 (48.24)	603 (87.48)	8.14	7.69
13L	300	345 (49.97)	614 (89.07)	8.30	6.83
14L	400	324 (47.01)	470 (68.22)	5.14	6.88
15L	500	332 (48.12)	479 (69.48)	10.92	11.09
16L	600	326 (47.28)	410 (59.53)	27.34	45.95
17L	700	205 (29.71)	248 (35.98)	64.30	71.69
18L	800	106 (15.34)	119 (17.31)	112.66	72.25

Table 18. Tensile properties on 0.76-mm sheet specimens of 7.5-kg (15-lb) heat (13998) of FA-362 alloy. The heat was melted by the air-induction-melted process and cast into a 72-mm-diam ingot. The ingot was extruded at 1000°C in a mild steel wrap into a rectangular cross section. The extruded cross section was hot rolled in a steel cover at 900°C to 0.76-mm-thick sheet. The sheet was stress relieved at 700°C for 1 h, followed by oil quenching. The punched specimens were annealed for 1 h at 700°C, followed by oil quenching.

Specimen	Test temperature (°C)	Strength, MPa (ksi)		Ductility, %	
		Yield	Ultimate tensile	Total elongation	Reduction of area
1L	24	351 (50.87)	569 (82.5)	6.30	4.38
2L	24	386 (55.96)	636 (92.3)	6.36	9.15
3L	100	358 (51.88)	478 (69.33)	2.56	4.13
16L	100	336 (48.71)	449 (65.18)	3.00	10.12
4L	200	357 (51.73)	677 (98.15)	8.60	7.23
5L	300	396 (57.38)	643 (93.27)	7.40	5.80
6L	400	346 (50.23)	464 (67.27)	3.50	9.48
7L	500	365 (53.00)	424 (61.53)	2.00	3.20
8L	600	297 (43.02)	381 (55.25)	21.30	27.95
9L	700	223 (32.30)	260 (37.77)	24.10	32.64
10L	800	93 (13.55)	132 (19.10)	66.30	57.58

ORNL-DWG 92-11981

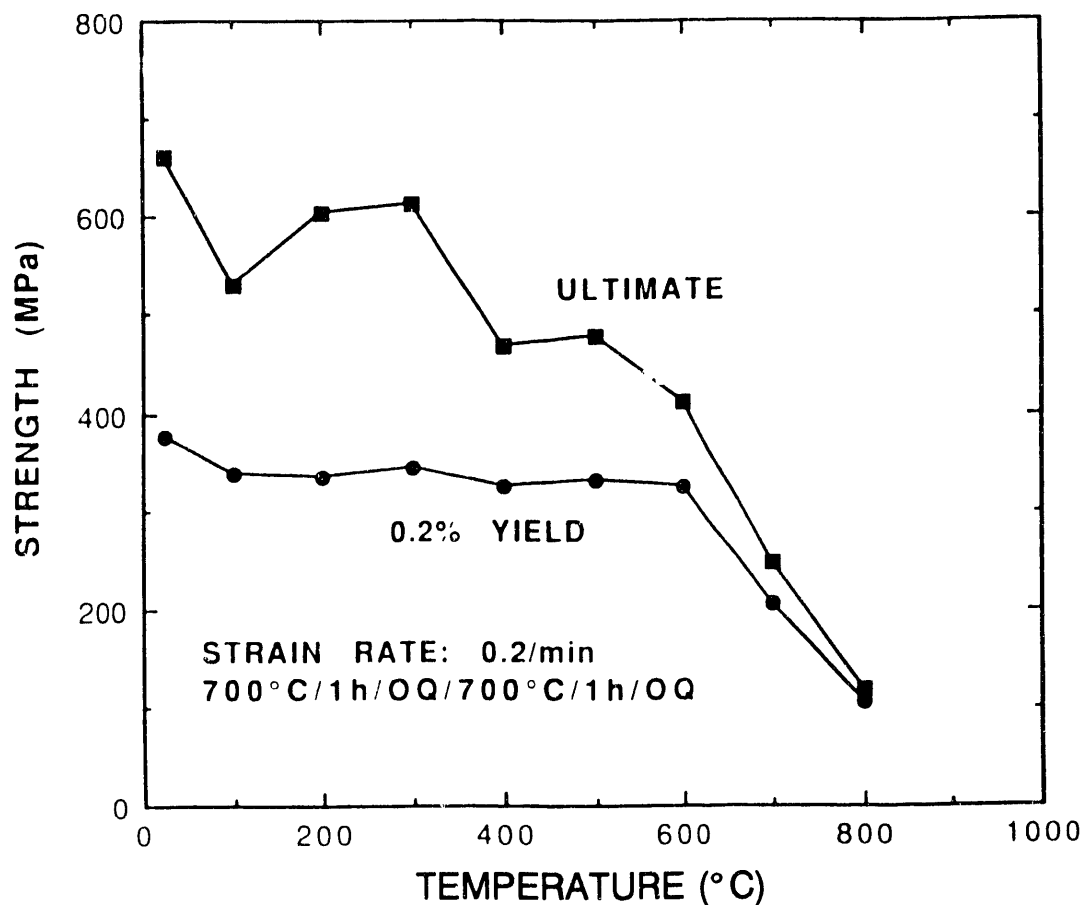


Fig. 25. Plot of yield and ultimate tensile strength as a function of test temperature for sheet specimens of FA-350. The sheet was stress relieved at 700°C for 1 h, followed by oil quenching prior to punching specimens. The specimens were given an annealing treatment at 700°C for 1 h, followed by oil quenching prior to tensile testing. All of the tests were in air at a strain rate of 0.2/min ( $3.33 \times 10^{-3}$ /s).

ORNL-DWG 92-11982

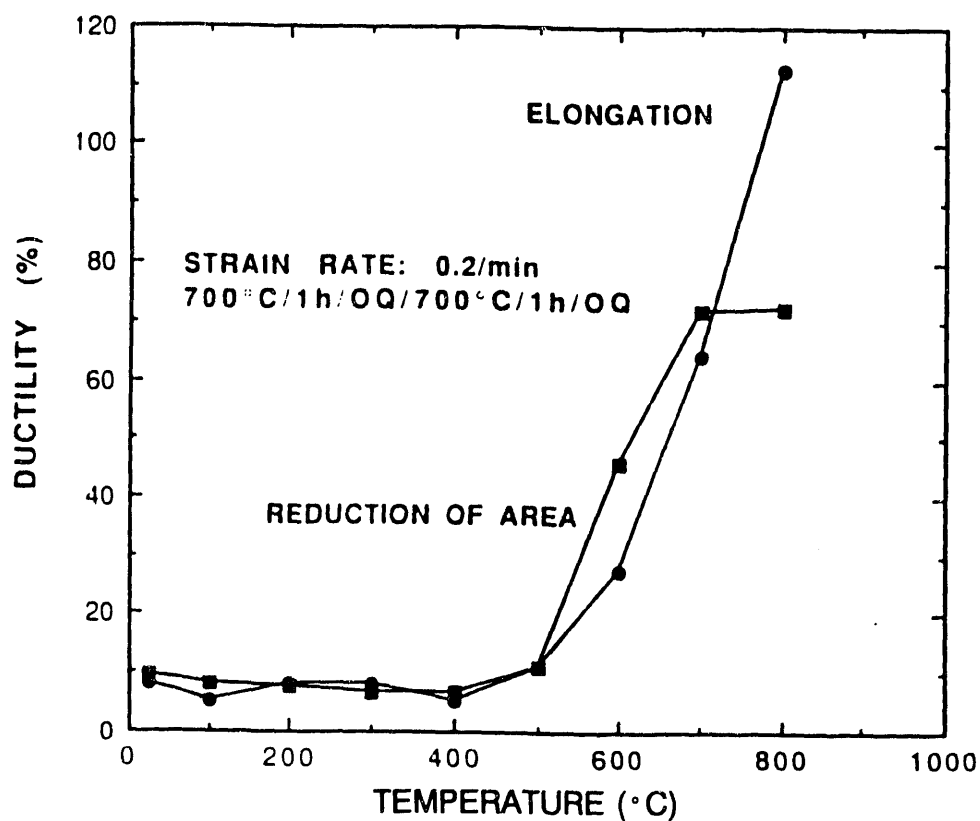


Fig. 26. Plot of total elongation and reduction of area as a function of test temperature for sheet specimens of FA-350. The sheet was stress relieved at 700°C for 1 h, followed by oil quenching prior to punching specimens. The specimens were given an annealing treatment at 700°C for 1 h, followed by oil quenching prior to tensile testing. All of the tests were in air at a strain rate of 0.2/min ( $3.33 \times 10^{-3}/s$ ).

ORNL-DWG 92-11983

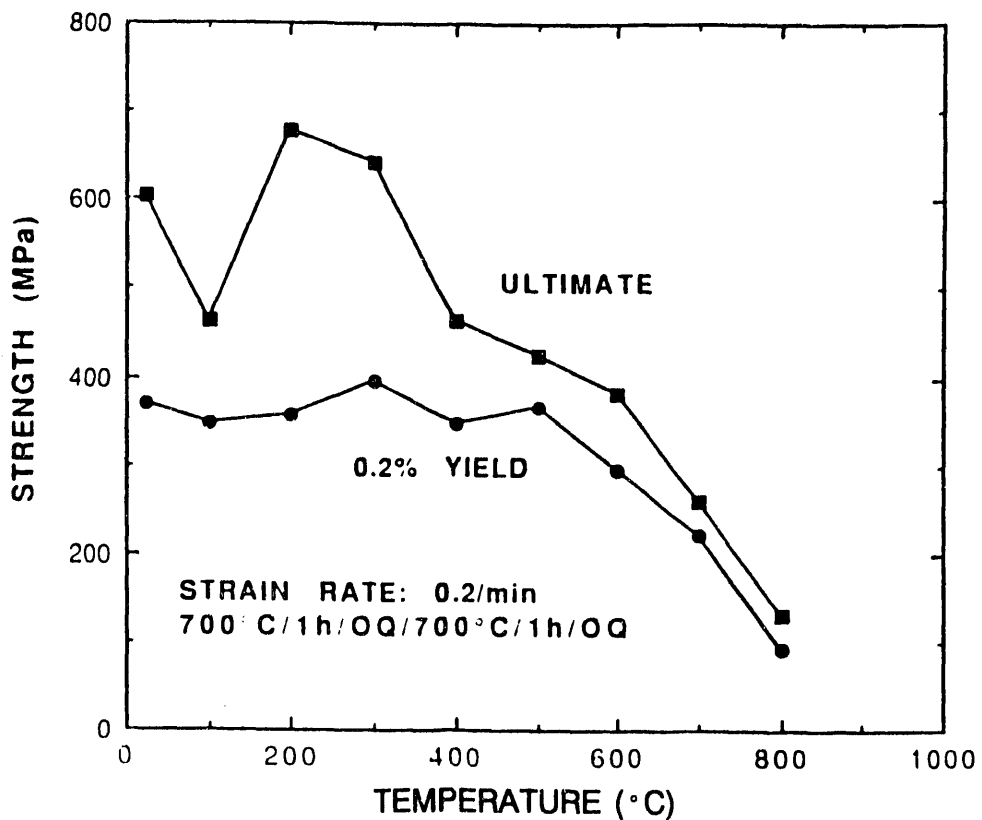


Fig. 27. Plot of yield and ultimate tensile strength as a function of test temperature for sheet specimens of FA-362. The sheet was stress relieved at 700°C for 1 h, followed by oil quenching prior to punching specimens. The specimens were given an annealing treatment at 700°C for 1 h, followed by oil quenching prior to tensile testing. All of the tests were in air at a strain rate of 0.2/min ( $3.33 \times 10^{-3}$ /s).

ORNL-DWG 92-11984

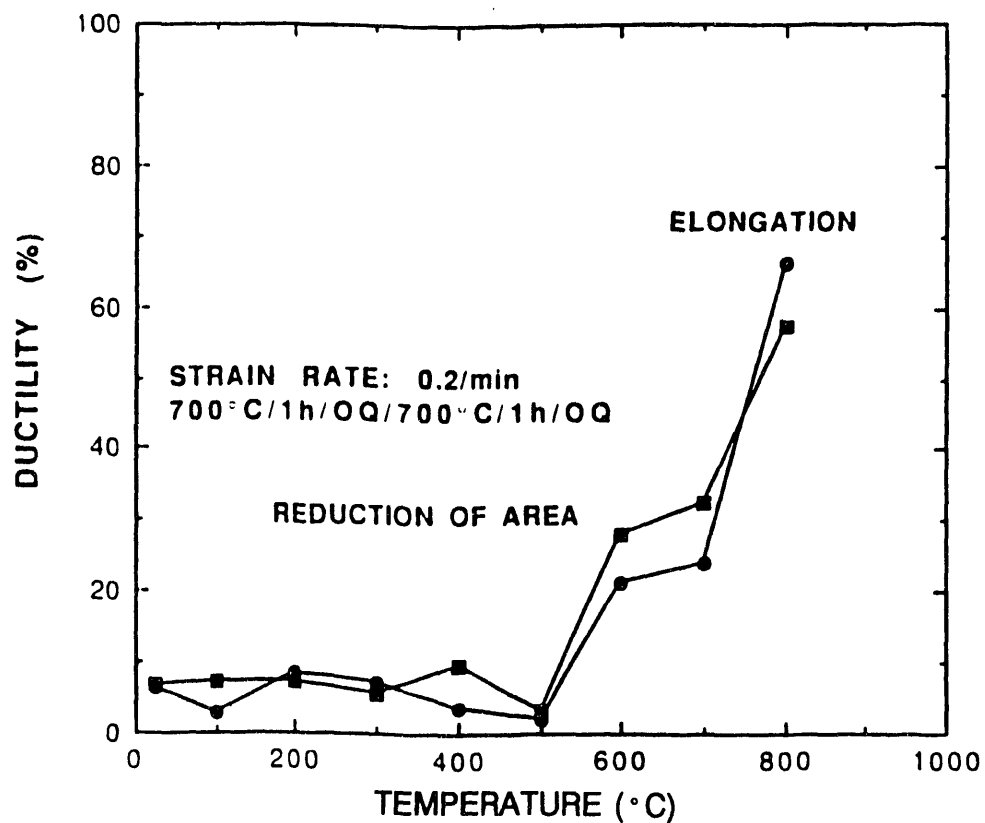


Fig. 28. Plot of total elongation and reduction of area as a function of test temperature for sheet specimens of FeAl alloy FA-362. The sheet was stress relieved at 700°C for 1 h, followed by oil quenching prior to punching specimens. The specimens were given an annealing treatment at 700°C for 1 h, followed by oil quenching prior to tensile testing. All of the tests were in air at a strain rate of 0.2/min ( $3.33 \times 10^{-3}$ /s).

ORNL-DWG 92-11985

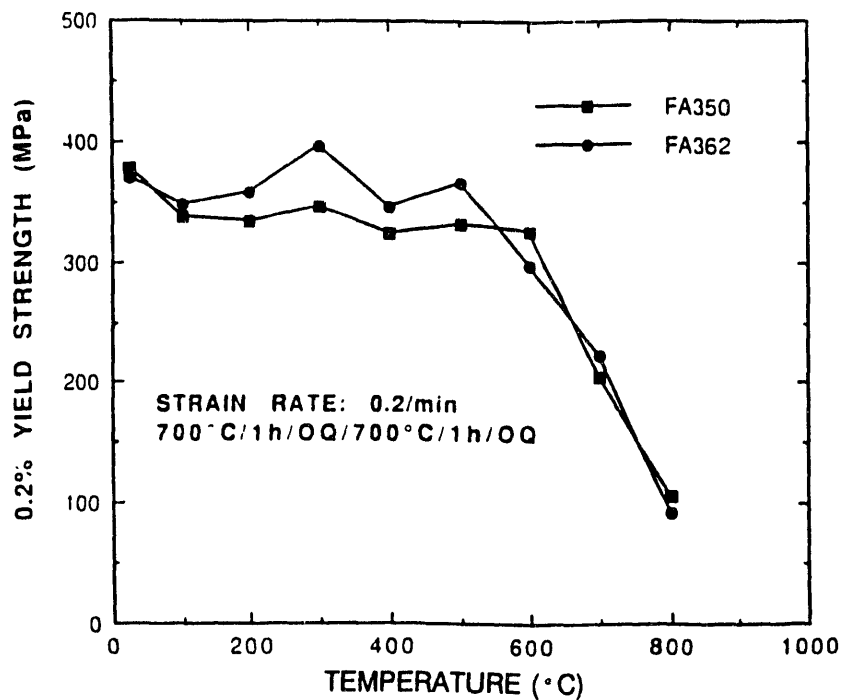


Fig. 29. Comparison of yield strength of FA-350 and -362 in sheet form as a function of test temperature.

ORNL-DWG 92-11986

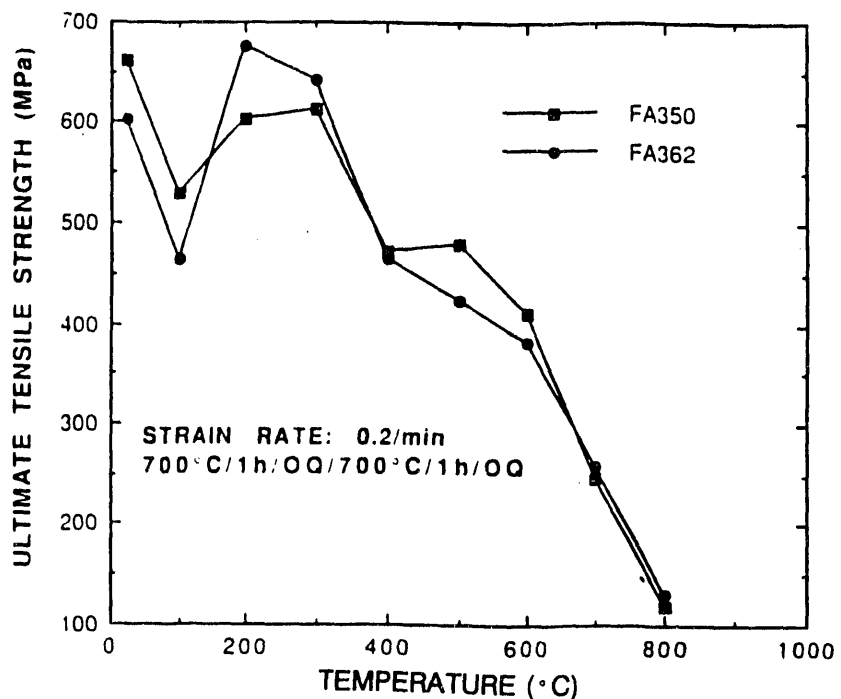


Fig. 30. Comparison of ultimate tensile strength of FA-350 and -362 in sheet form as a function of test temperature.

ORNL-DWG 92-11987

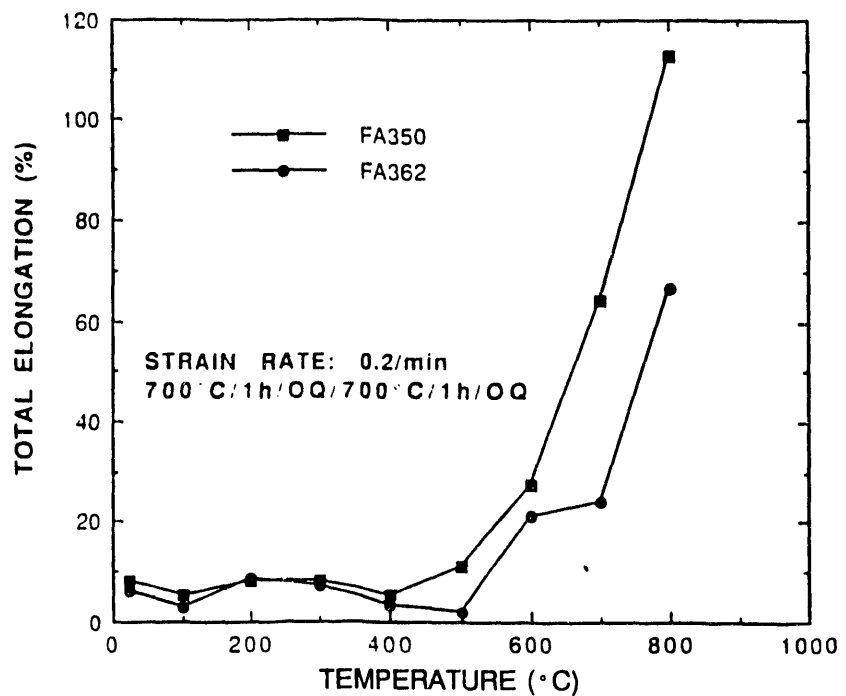


Fig. 31. Comparison of total elongation of FA-350 and -362 in sheet form as a function of test temperature.

ORNL-DWG 92-11988

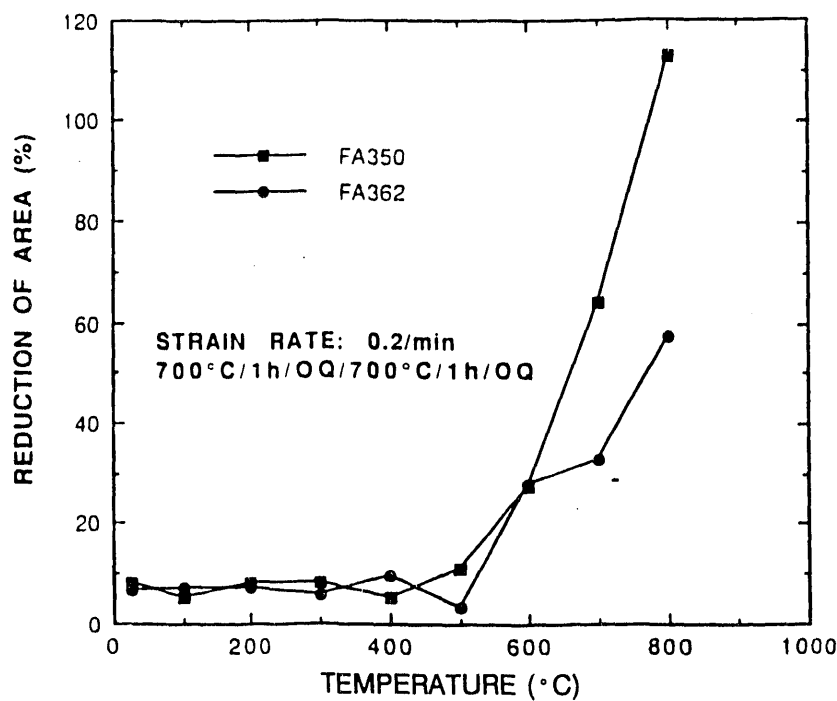


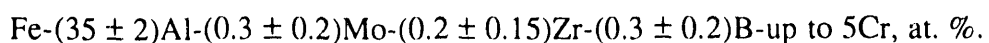
Fig. 32. Comparison of reduction of area of FA-350 and -362 in sheet form as a function of test temperature.

rolling at temperatures of 1100 to 900°C. Tensile tests show a general trend of increase in yield strength with aluminum at temperatures to 400°C. The strength becomes insensitive to the aluminum concentration at 600°C, and it shows a general decrease with aluminum at 700°C. The tensile elongation generally decreases with the aluminum level when tested at temperatures to 400°C. At higher temperatures, the alloys exhibit a peak ductility around 35 to 38% Al. FeAl starts to show brittle grain-boundary fracture as its aluminum level reaches 38%. Binary FeAl alloys were weak in creep resistance. Our studies, together with the corrosion investigation,<sup>12</sup> led to the selection of Fe-35.8% Al as the base composition for alloy development.

Alloy development was focused on improving room-temperature ductility and elevated-temperature strength and creep resistance. Boron and zirconium were found to lower the yield strength and to improve the tensile ductility of FeAl (35.8% Al) at room temperature. When both elements were present, they reacted to form ZrB<sub>2</sub>, as revealed by electron microprobe analyses. The beneficial effect is therefore only detected when the B/Zr ratio is larger than two. Additions of chromium to FeAl alloys do not improve their room-temperature ductility. Refinement of the grain structure by hot extrusion, on the other hand, substantially improves the tensile ductility of FeAl alloys.

Additions of vanadium and molybdenum enhance the strength of FeAl alloys. Vanadium at a level of 0.5% substantially improves the yield and ultimate tensile strengths at room temperature and 600°C. Alloying with 0.2% Mo increases both strength and ductility of FeAl alloys at room and elevated temperatures. The alloy FA-362 (Fe-35.8Al-0.2Mo-0.05Zr-0.24B, at. %) has a room-temperature tensile ductility of 11.8%, the highest tensile ductility ever reported for FeAl. Most important, molybdenum at 0.2% substantially extends the rupture life and reduces the creep rate of FeAl tested at 593°C and 138 MPa. Further increases in molybdenum concentration cause a decrease in ductility and strength at room temperature, and creep resistance at elevated temperatures. A combination of 0.5% Mo and 5% Cr also improves creep properties of FeAl alloys. The alloy with 0.2% Mo had improved oxidation resistance at 1000°C.

Our alloying effort has led to identification of the following aluminide composition with promising properties:



However, this composition is likely to be modified in future work to improve weldability of the alloy. In the alloys, boron and zirconium are added for ductility

improvement at ambient temperatures and molybdenum and chromium for strength and creep improvement at elevated temperatures.

The melting of scaled-up heats was conducted for selected FeAl alloys with improved properties. The scaled-up heats of 7.5-, 40-, and 250-kg (15-, 80-, and 500-lb) sizes were melted by AIM, VIM, and ESR processes. The ingot sizes varied from 72 to 205 mm (2.85 to 8 in.). Scaled-up heats were melted at ORNL, Haynes International, and The Timken Company. The heats were fabricated by hot forging, hot extruding, and hot rolling. Products fabricated were round and rectangular bar, sheet, and tubing. The microstructures of various product forms from the scaled-up heats were also determined. The following conclusions at this time are:

1. AIM of scaled-up heats to good quality ingots is possible if the melt stock of iron and aluminum is deoxidized and dehydrated properly. Regular melt stock produced ingots with large gas porosity. VIM is an acceptable scaled-up method for good quality ingots for regular melt stock. The ESR process further enhances the quality of the ingots. However, the benefit of ESR on mechanical properties has not yet been determined.
2. Heating the dies and work piece to the same temperature allowed a broad range of forging temperatures (800 to 1000°C) for arc-melted heats. Without heating the dies, scaled-up ingots could not be forged in the as-cast condition. Worked structure produced by hot extruding the ingots could be hot forged at 1000°C without heating the dies.
3. Good quality extrusions of scaled-up ingots could be produced only by wrapping the ingot in a mild steel sheet or a can. Extrusion temperatures ranged from 900 to 1100°C. Extrusions of round, rectangular, and tubular shapes were possible.
4. Hot rolling of the forged or extruded structure from the scaled-up heats was possible only in a steel cover. The rolling temperatures varied between 800 to 900°C.
5. The cover for extruding and rolling of heated dies for forging is needed to keep the surface temperature of the work piece in the high-ductility region. The high-ductility region for FeAl alloys was determined to be above 600°C for the hot-rolled sheet. The same temperature for coarse-grain cast ingot is expected to be even higher.
6. The yield strength of the scaled-up heats remained constant up to 600°C. The ultimate-tensile-strength values were directly related to ductility in the temperature range of room temperature to 600°C.
7. The mechanical properties of the scaled-up FA-350 heats are comparable to those of the small research heat (400 g), whereas the ductility and strength of the scaled-up FA-362

heat are generally lower. A factor that may contribute to the difference in properties is that the scaled-up heat was prepared by AIM in air (containing moisture), whereas the small research heat was prepared by arc melting in an inert gas atmosphere.

8. Scale-up of these alloys is possible. However, special care will be necessary in selecting the melt stock, melting practice, and processing the ingots. Cutting and machining of the ingots will also require attention.
9. The present studies have identified conditions for processing the scaled-up heats.

However, thermomechanical processing optimization of the scaled-up heats needs further study to achieve the maximum ductility potential of FeAl alloys.

## 8. ACKNOWLEDGMENTS

The authors are grateful to P. F. Tortorelli, E. P. George, and J. H. DeVan for paper review and valuable discussions and E. H. Lee, D. H. Pierce, T. J. Henson, J. D. Vought, K. S. Blakely, L. M. Pike, and P. A. Ferguson for technical assistance. Thanks are also due to Connie Dowker and M. L. Atchley for manuscript preparation, Marcia Hodges for final report preparation, and K. Spence for editing.

## 9. REFERENCES

1. *Binary Alloy Phase Diagrams*, ed. T. B. Massalski, Vols. 1 and 2, American Society for Metals, Materials Park, Ohio, 1986.
2. B. Schmidt, P. Nagpal, and I. Baker, pp. 755-60 in *High-Temperature Ordered Intermetallic Alloys III*, proceedings of Materials Research Society Symposium, Vol. 133, ed. C. T. Liu, A. I. Taub, N. S. Stoloff, and C. C. Koch, Materials Research Society, Pittsburgh, 1989.
3. J. L. Smialek, J. Doychak, and D. J. Gaydosh, *Oxidation Behavior of FeAl + Hf,Zr,B*, NASA TM-101402, NASA Lewis Research Center, Cleveland, September 1988.
4. C. G. McKamey et al., *Evaluation of Mechanical and Metallurgical Properties of Fe<sub>3</sub>Al-Based Aluminides*, ORNL/TM-10125, Martin Marietta Energy Systems, Inc., Oak Ridge Natl. Lab., September 1986.

5. J. H. DeVan, Martin Marietta Energy Systems, Inc., Oak Ridge Natl. Lab., unpublished data, June 1990.
6. I. Baker and D. J. Gaydosh, *Mater. Sci. Eng.* **96**, 147 (1987).
7. M. G. Mendiratta, S. K. Ehlers, and D. K. Chatterjee, p. 420 in *Proceedings of the National Bureau of Standards Symposium, Rapid Solidification Processing: Principles and Technologies, December 6-8, 1982*, National Bureau of Standards, Gaithersburg, Md., 1983.
8. J. A. Horton, C. T. Liu, and C. C. Koch, pp. 309-21 in *High-Temperature Alloys: Theory and Design*, ed. J. O. Stiegler, The Metallurgical Society of AIME, Warrendale, Pa., 1984.
9. D. J. Gaydosh, S. L. Draper, and M. V. Nathal, *Metall. Trans. A* **20A**, 1701 (1989).
10. V. K. Sikka, C. G. McKamey, C. R. Howell, and R. H. Baldwin, *Fabrication and Mechanical Properties of Fe<sub>3</sub>Al-Base Iron Aluminides*, ORNL/TM-11465, Martin Marietta Energy Systems, Inc., Oak Ridge Natl. Lab., March 1990.
11. P. F. Tortorelli, P. S. Bishop, and J. R. DiStefano, *Selection of Corrosion-Resistant Materials for Use in Molten Nitrate Salts*, ORNL/TM-11162, Martin Marietta Energy Systems, Inc., Oak Ridge Natl. Lab., October 1989.
12. P. F. Tortorelli and P. S. Bishop, *Influences of Compositional Modifications on the Corrosion of Iron Aluminides by Molten Nitrate Salt*, ORNL/TM-11598, Martin Marietta Energy Systems, Inc., Oak Ridge Natl. Lab., October 1990.
13. P. F. Tortorelli and P. S. Bishop, "Corrosion of Aluminides by Molten Nitrate Salt," to be published in *Environmental Effects on Advanced Materials*, proceedings of The Metallurgical Society of AIME, TMS-AIME, New York, 1990.
14. *High-Temperature Ordered Intermetallic Alloys*, proceedings of the Materials Research Society Symposium held at Boston, Maine, Vol. 39, ed. C. C. Koch, C. T. Liu, and N. S. Stoloff, Materials Research Society, Pittsburgh, 1985.
15. *High-Temperature Ordered Intermetallic Alloys II*, proceedings of the Materials Research Society Symposium held at Boston, Maine, Vol. 81, ed. C. C. Koch, C. T. Liu, and O. Izumi, Materials Research Society, Pittsburgh, 1987.
16. *High-Temperature Ordered Intermetallic Alloys III*, proceedings of the Materials Research Society Symposium, Vol. 133, ed. C. T. Liu, A. I. Taub, N. S. Stoloff, and C. C. Koch, Materials Research Society, Pittsburgh, 1989.
17. C. G. McKamey, J. A. Horton, and C. T. Liu, *Scr. Metall.* **22**, 1679 (1988).
18. C. G. McKamey, J. A. Horton, and C. T. Liu, *J. Mater. Res.* **4**, 1156-63 (1989).

19. C. T. Liu, E. H. Lee, and C. G. McKamey, *Scr. Metall.* **23**, 875 (1989).
20. C. T. Liu, C. G. McKamey, and E. H. Lee, *Scr. Metall.* **24**(2), 385 (1990).
21. C. T. Liu and E. P. George, *Scr. Metall.* **24**, 1285-90 (1990).
22. C. G. McKamey et al., "Development of Iron Aluminides for Coal Conversion Systems," ORNL/TM-10793, Martin Marietta Energy Systems, Inc., Oak Ridge Natl. Lab., July 1988.
23. C. G. McKamey, J. A. Horton, and C. T. Liu, pp. 321-27 in *High-Temperature Ordered Intermetallic Alloys II*, Vol. 81, proceedings of the Materials Research Society Symposium, held at Boston, Maine, ed. N. S. Stoloff, C. C. Koch, C. T. Liu, and O. Izumi, Materials Research Society, Pittsburgh, 1987.
24. M. A. Crimp and K. Vedula, *Mater. Sci. Eng.* **78**, 193 (1986).
25. K. Vedula and J. R. Stephens, pp. 381-91 in *High-Temperature Ordered Intermetallic Alloys II*, proceedings of the Materials Research Society Symposium held at Boston, Maine, Vol. 81, ed. C. C. Koch, C. T. Liu, and O. Izumi, Materials Research Society, Pittsburgh, 1987.
26. J. H. DeVan and C. A. Hippsley, pp. 31-40 in *Oxidation of High-Temperature Intermetallics*, ed. T. Grobstein and Doychak, The Metallurgical Society of AIME, TMS-AIME, New York, 1989.

**INTERNAL DISTRIBUTION**

1-2. Central Research Library	33-37. C. T. Liu
3. Document Reference Library	38. K. C. Liu
4-5. Laboratory Records Department	39. A. S. Loebel
6. Laboratory Records, ORNL-RC	40. R. A. Lowden
7. ORNL Patent Section	41. G. M. Ludtka
8-10. M&C Records Office	42. G. M. Ludtka
11. D. J. Alexander	43. N. Manly
12. J. D. Allen, Jr.	44. J. R. Mayotte
13. P. Angelini	45. P. J. Maziasz
14. H. G. Arnold	46-50. C. G. McKamey
15. P. F. Becher	51. R. N. Morris
16. R. A. Bradley	52. P. L. Rittenhouse
17. C. R. Brinkman	53. J. H. Schneibel
18. R. S. Carlsmith	54-58. V. K. Sikka
19. N. C. Cole	59. P. S. Sklad
20. D. F. Craig	60. G. M. Slaughter
21. J. H. DeVan	61. C. J. Sparks
22. E. P. George	62. V. J. Tennery
23. G. M. Goodwin	63. P. F. Tortorelli
24. R. L. Heestand	64. S. Viswanathan
25. J. A. Horton, Jr.	65. J. R. Weir
26. L. L. Horton	66. Y. A. Chang (Consultant)
27. T. J. Huxford	67. H. W. Foglesong (Consultant)
28. R. R. Judkins	68. J. J. Hren (Consultant)
29. J. R. Keiser	69. M. L. Savitz (Consultant)
30. J. F. King	70. J. G. Simon (Consultant)
31. W. Y. Lee	71. K. E. Spear (Consultant)
32. H. Lin	

**EXTERNAL DISTRIBUTION**

72. CARPENTER TECHNOLOGY CORPORATION, 101 West Bern St.,  
P.O. Box 4662, Reading, PA 19612-4662

N. Fiore

73. COORS CERAMIC COMPANY, Technical Operations and Engineering,  
600 Ninth St., Golden, CO 80401

D. Wirth, Vice President

74. DARTMOUTH COLLEGE, Thayer School of Engineering, Hanover, NH 03755

I. Baker

75. DOW CHEMICAL COMPANY, INC., Central Research, Catalysis Laboratory,  
1776 Building, Midland, MI 49674

R. D. Varjian

76. ELECTRIC POWER RESEARCH INSTITUTE, Nuclear Plant Corrosion Control,  
3412 Hillview Ave., Palo Alto, CA 94303

M. M. Behravesh

77. LEHIGH UNIVERSITY, Bethlehem, PA 18015

A. K. MacPherson

78-79. LOS ALAMOS NATIONAL LABORATORY, P.O. Box 1663, G771,  
Los Alamos, NM 87545

J. J. Petrovic  
A. D. Rollett

80. NATIONAL INSTITUTE OF STANDARDS AND TECHNOLOGY, Metallurgy  
Division, Building 223, Room B248, Gaithersburg, MD 20899

R. E. Ricker

81. NAVAL RESEARCH LABORATORY, Materials Science Component Technology,  
Code 6000, Building 43, Room 212, Washington, DC 20385-5000

B. B. Rath, Associate Director of Research

82. NORTH CAROLINA STATE UNIVERSITY, Department of Materials Engineering,  
Yarborough Dr., Raleigh, NC 27695-7907

C. C. Koch

83. UNIVERSITY OF CINCINNATI, Materials Science and Engineering Department,  
ML 012, Cincinnati, OH 45221

J. A. Sekhar

84. UNIVERSITY OF TENNESSEE, Department of Materials Science and Engineering,  
Knoxville, TN 37996-2200

B. F. Oliver

85. VANDER LINDEN AND ASSOCIATES, 5 Brassie Way, Littleton, CO 80123

C. R. Vander Linden

86. WISCONSIN CENTRIFUGAL, 905 E. St. Paul Ave., Waukesha, WI 53188-3898

T. J. Devine

87-88. U.S. DOE, Forrestal Building, 1000 Independence Ave., SW, Washington,  
DC 20585

M. E. Gunn, Jr. (CE-232)  
P. H. Salmon-Cox

89. U.S. DOE, ADVANCED INDUSTRIAL CONCEPTS DIVISION, Advanced Industrial  
Concepts Materials Program, 1000 Independence Ave., S.W., Washington,  
DC 20585

C. A. Sorrell (CE-232)

90. U.S. DOE, OFFICE OF INDUSTRIAL TECHNOLOGIES, Forrestal Building,  
1000 Independence Ave., Washington, DC 20585

S. L. Richen, Program Manager (CE-221)

91-92. U.S. DOE, OAK RIDGE FIELD OFFICE, P.O. Box 2008, Oak Ridge,  
TN 37831

Deputy Assistant Manager for Energy Research and Development  
E. E. Hoffman

93-94. U.S. DOE, OFFICE OF SCIENTIFIC AND TECHNICAL INFORMATION,  
P.O. Box 62, Oak Ridge, TN 37831

For distribution by microfiche as shown in DOE/OSTI-4500,  
Distribution Category UC-310 [Industrial Programs (General)]

**DATE  
FILMED**

**8 / 19 / 93**

**END**

